Dynamics of Prestressed Concrete Railway Bridges

by

Sergio Ruiz Meléndez

B. Tech (Structural Engineering) 1998, U.P.V. Bilbao, Spain
B. Tech (Industrial Engineering) 2000, U.A.X. Madrid, Spain

SUBMITTED TO THE DEPARTMENT OF CIVIL AND ENVIRONMENTAL ENGINEERING IN PARTIAL FULFILLMENT OF THE REQUIREMENTS FOR THE DEGREE OF

MASTER OF ENGINEERING IN CIVIL AND ENVIRONMENTAL ENGINEERING

at the

MASSACHUSETTS INSTITUTE OF TECHNOLOGY

June 2001

Author .....
Department of Civil and Environmental Engineering
May 11th, 2001

Certified by .....
Jerome Connor
Professor of Civil and Environmental Engineering
Thesis Supervisor

Accepted by .....
Oral Buyukozturk
Chairman, Department Committee on Graduate Students

DYNAMICS OF PRESTRESSED CONCRETE RAILWAY BRIDGES

by

Sergio Ruiz Meléndez

Submitted to the Department of Civil and Environmental Engineering on May 11, 2001
in partial fulfillment of the requirements for the degree of

Master of Engineering in Civil and Environmental Engineering

Abstract

The purpose of this thesis is to evaluate the dynamic displacement effects of a Prestressed concrete bridge while a high-velocity train is traveling along it.

High Speed Railways require a high linearity, with large radius of curvature on curves and limited slope. In order to satisfy these requirements, large percentages of the total projects have to be done with the rails lying on bridges, viaducts or just elevated.

Prestressed concrete has been proved, from many projects constructed all over the world for the last 20 years, to be one of the most effective structural design choices in terms of economy, constructibility, maintainability and expected life cycle. Because of it, this structural system will be the one to be used in order to perform the current study on the effects that the dynamic loadings, from high-speed trains, would produce on such bridge type structures.

Basic principles of prestressed concrete will be covered in order to be able to perform the dynamic analysis as well as to determine the dynamic impact that the train traveling along a bridge would produce on it by doing a motion based design.

Basic concepts of bridge dynamic analysis will also be covered. Since the vehicle speed is the most important parameter influencing the dynamic stresses and deflections, and because they generally increase with increasing speed, the analysis of its effects on bridges is extremely important in order to be able to upgrade the performance of the structures.

Once all the required concepts for the prestressed concrete beam dynamic analysis have been reviewed a case study will be performed. Since the large deflections caused by the dynamic load impact can increase environmental noise and the track maintenance required and decrease the ride comfort quality for the passengers, is the purpose of the above mentioned study to determine those deflections at all times so that we may determine when, where, and why should we take actions in order to limit them.

Thesis Supervisor: Jerome Connor
Title: Professor of Civil and Environmental Engineering

To Neretxo

1. High Speed Railway for the 21st Century.

Hundreds of miles of high velocity railways have been constructed all over world in the past 20 years, and many others are projected for a nearby future. The reason why the transportation authorities are looking in this direction is the search of several important purposes like the improvement the overcrowded traffic condition along the areas they cover, the increase of the value of the land use and development, the upgrade of the living quality and standard, and the acceleration of the economic development, growth, etc.

Moreover this technologically advanced transportation system ables passenger trains to reach speeds up to 250 km/h (155 mph). However it is expected that railway traffic based on the principle of wheels rolling along rails has a maximum speed of 500 km/h (315 mph). Therefore, further development includes magnetically levitated (MAGLEV) vehicles which will attain even higher speeds.

1.1. High-Velocity in Europe. The German case.

France, Italy, United Kingdom, Spain and Germany are some of the countries that more invested in this technologically advanced transportation system in Europe in the last 20 years.

In the German case, 250 km/h (155mph) passenger trains have been designed with the result of maximum slopes of 12.5% minimum radius of 7,000 m.

We may appreciate the important role bridges play for this type of infrastructures taking a look to the first two railways connecting Hannover with Wurzburg, of 327 km and Manheim with Stuttgart, of 99 km, both crossing mountainous areas, and in which

130 km of tunnels were built and 35 km were bridges, what represents an 8% of the total.

In Germany, prestressed concrete has been chosen most of the times for the construction of high-speed line bridges and viaducts because of its economy comparing to its equivalent in steel for approximate spans. It was considered the possibility of replacing the decks in a period of time between 80 and 150 years after construction by removing them transversally, what made them to limit the span of the continuous viaducts. In order to do this, they have often been using isostatic beams. The average span used was 44 m and the maximum spans constructed were of 58 m. However, in many cases, they have taken the aesthetical, structural and the constructibility advantages of the continuous beam bridges. This advantages are between others hiperstaticity, lower deformations, possibility of high quality construction by using the bridge launching procedure, slimmer piles and decks that would make the structure to be more integrated in the landscape. However, it will be described in much more detail the advantages of both, simple span and continuous bridges, in terms of design and constructibility.

1.2. High-Velocity in the US.

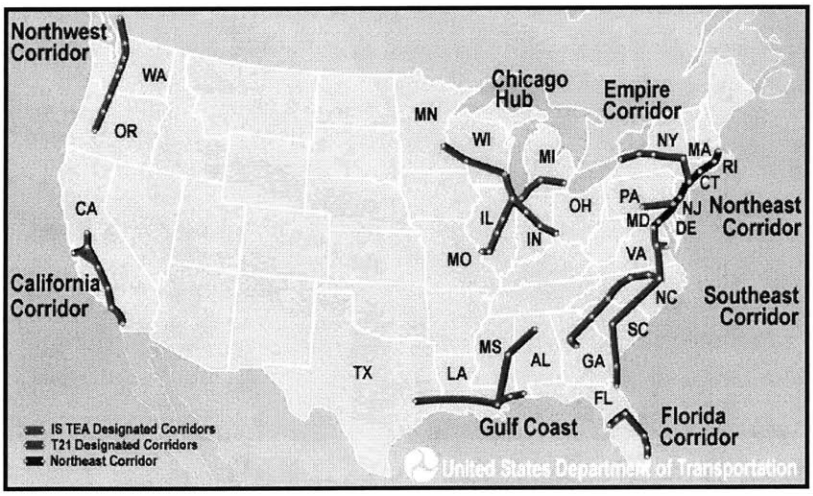

Figure 1.1

In the United States, after many decades of decline, the rail industry is gathering steam again. Although this is mostly due to the increase on the construction of light-rail networks in many metropolitan areas all over the country, it is also because of the many high-speed rail lines already constructed, being constructed of just projected.

An example of an already constructed high-speed line is the one called Northeast Corridor, which connects Boston with New York City, and that will continue to Washington DC in a nearby future. Examples of projected high-velocity lines are the one named Northwest Corridor, which will revamp track between Seattle, Vancouver and British Columbia or the Alameda Corridor in California, connecting Los Angeles with Long Beach.

Because the US has a high geographical diversity, the design and construction options vary significantly for each case. Hence, the line connecting Boston with New York only had to be adapted to the high-velocity circulation while in the Northwest corridor, because it is a highly mountainous area, similar design and construction options, like the ones taken in Germany, should be taken as the optimal in terms of economy, constructibility and maintainability.

1.3. High-Velocity in Asia.

There are many high-speed rails already constructed in Asia, most of them in Japan. One example of the magnitude of the projects done in Japan is the Kojima-Sakaide Route, a 13.1 km series of bridges across the Inland Sea. The route connects two of Japan's four main islands, Honshu and Shikoku. The route skips between five islands and contains five double decker bridges. It took 20 years to design and nine years to build and was opened on 1989.

Design had to counter earthquake movements and typhoon winds. The upper deck contains four highway lanes and the lower deck carries two high speed rail lines. Moreover, design of the route required writing construction standards, as Japan had no long-span bridges in the 1950s.

In Taiwan, the total length of the route of the high-speed railway being constructed at the moment from Taipei, at the North of the country, to Kaohsiung, and industrial and harbor city in the south, is of about 345 km. In order to save money for land and time for construction, most parts of the route are on elevated railway. Simple-span beams and three-equal-span continuous reinforced-concrete beams supported on piers are the two most important standard design types used.

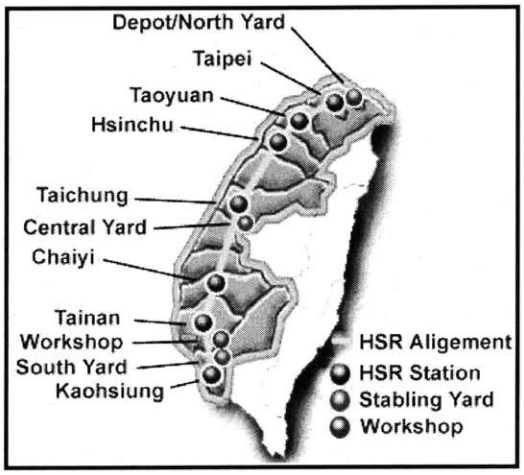

Figure 1.2

2. Prestressed Concrete.

2.1. Prestressed Concrete evolution.

Prestressed concrete began to acquire importance about right after the Second World War. Perhaps the shortage of steel in Europe during the war had given it some impetus, since much less steel is required for prestressed concrete than for conventional types of construction. But it must also be realized that time was needed to prove and improve the serviceability, economy, and safety of prestressed concrete as well as to acquaint engineers and builders with a new method of design and construction.

Although France and Belgium led the development of prestressed concrete, England, Germany, Switzerland, Holland, Soviet Russia, and Italy quickly followed. Since 1965, about 47% of all bridges built in Germany were of prestressed concrete. Since the late 1960s and 1970s most medium-span bridges (100-300 ft, 30-90 m) and many long-span bridges up to about 1000 ft (305 m) were built of prestressed concrete in all parts of the world.

Prestressed concrete in the United States did not start until 1949 and since 1960, the use of prestressed concrete bridges has become a standard practice. In many of the states almost all bridges in the span range 60 to 120 ft (18-36 m) have been constructed with prestressed concrete. Since the late 1970s, post-tensioned bridges of medium spans (150-650 ft, 45-200 m) have gained momentum, in the form of continuous or cantilever construction.

2.2. Basic concepts of prestressing

Prestressed concrete construction systems are those in which an internally or externally compressive force p is induced on the structural element in order to maximize the utilization of reinforced concrete, weak in tension but strong in compression. This compressive force is applied through the use of stressed high-strength prestressing wires or tendons prior to loading and because of this, the concrete section is generally stressed only in compression under service and sometimes overload conditions.

It is important for the designer to fully understand the different prestressed concrete design concepts so that he or she can proportion and design those structures with intelligence and efficiency.

The Prestressing to transform concrete into an elastic material is a very extended concept, which is the one to be considered at the case study, is explained as follows.

Prestressing to Transform Concrete into an Elastic Material. This concept considers concrete as an elastic material and is probably still the most commonly adopted viewpoint among engineers. Was Eugene Freyssinet who visualized prestressed concrete as essentially concrete which is transformed from a brittle material into an elastic one by a previous compression applied to it. Concrete which is weak in tension and strong in compression is compressed (generally by steel under high tension) so that the brittle concrete would be able to withstand tensile stresses. From this concept the criterion of no tensile stresses was born. It is generally believed that if there are no tensile stresses in the concrete, there can be no cracks, and the concrete is no longer a brittle material but becomes an elastic material.

From this standpoint concrete is visualized as being subject to two systems of forces: internal prestress and external load, with the tensile stresses due to the external load counteracted by the compressive stresses due to the prestress. Similarly, the

cracking of concrete due to load is prevented or delayed by the precompression produced by the tendons. So long as there are no cracks, the stresses, strains, and deflections of the concrete due to the two systems of forces can be considered separately and superimposed if necessary.

In prestressed concrete, high-tensile steel is used which will have to be elongated a great deal before its strength is fully utilized. If the high-tensile steel is simply buried in the concrete, as in ordinary concrete reinforcement, the surrounding concrete will have to crack very seriously before the full strength of steel is developed. Hence it is necessary to prestretch the steel with respect to the concrete. By prestretching and anchoring the steel against the concrete, we produce desirable stresses and stains in both materials: compressive stresses and strains in concrete, and tensile stresses and stains in steel. This combined action permits the safe and economical utilization of the two materials which cannot be achieved by simply burying steel in the concrete as is done for ordinary reinforced concrete. In isolated instances, medium-strength steel has been used as simple reinforcement without prestressing, and the steel was specially corrugated for bond, in order to distribute the cracks. This process avoids the expenses for prestretching and anchoring high-tensile steel but does not have the desirable effects of precompressing the concrete and of controlling the deflections.

From this point of view, prestressed concrete is no longer a strange type of design. It is rather an extension and modification of the applications of reinforced concrete to include steels of higher strength. Because of this, prestressed concrete cannot perform miracles beyond the capacity of the strength of its materials. Although much ingenuity can be exercised in the proper and economic design of prestressed-concrete structures, there is absolutely no magic method to avoid the eventual necessity of carrying an external moment by an internal couple. And that internal

resisting couple must be supplied by the steel in tension and the concrete in compression, whether it be prestressed or reinforced concrete.

The prestressing force P that satisfies the particular conditions of geometry and loading of a given element is determined from the principles of mechanics and of stress-strain relationships. Sometimes simplification is necessary, as when a prestressed beam is assumed to be homogeneous and elastic. A comprehensive treatment of the subject of prestressed concrete may be found in Equation 1. Consider, then, a simply supported rectangular beam subjected to a concentric prestressing force P, as shown in Figure 2.1. The compressive stress on the beam cross section is uniform and has an intensity

$$f = -\frac{P}{A_c} \qquad (1)$$

where $A_c = b \cdot h$ is the cross-sectional area of a beam section of width b and total depth h. A minus sign is used for compression and a plus sign for tension throughout the text. Also, bending moments are drawn on the tensile side of the member. If external transverse loads are applied to the beam, causing a maximum moment M at midspan, the resulting stress becomes

$$f^t = -\frac{P}{A} - \frac{Mc}{I_g} \qquad (2)$$

$$f_b = -\frac{P}{A} + \frac{Mc}{I_g} \qquad (3)$$

where

f^t = stress at the top fibers

f_b = stress at the bottom fibers

c = ½ h for the rectangular section

I_g = gross moment of inertia of the section ($bh^3/12$ in this case)

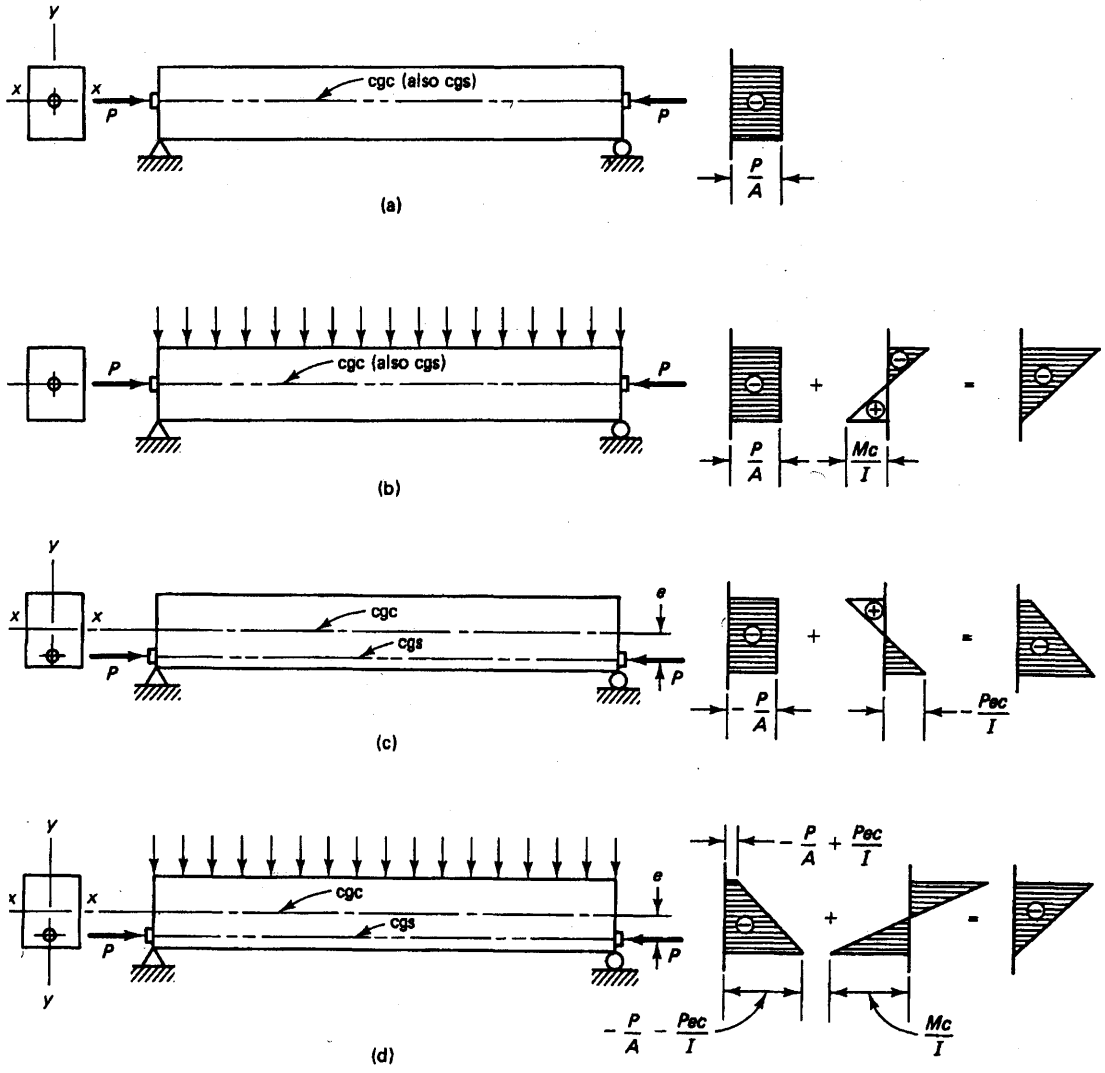

Figure 2.1

Equation 3 indicates that the presence of prestressing-compressive stress –P/A is reducing the tensile flexural stress Mc/I to the extent intended in the design, either eliminating tension totally (even inducing compression) or permitting a level of tensile stress within allowable code limits. The section is then considered uncracked and behaves elastically: the concrete's inability to withstand tensile stresses is effectively compensated for by the compressive force of the prestressing tendon.

The compressive stresses in equation 2 at the top fibers of the beam due to prestressing are compounded by the application of the loading stress –Mc/I, as seen in Figure 2. Hence the compressive stress capacity of the beam to take a substantial external load is reduced by the concentric prestressing force. In order to avoid this limitation, the prestressing tendon is placed eccentrically below the neutral axis at midspan, to induce tensile stresses at the top fibers due to prestressing (Figures 3 and 4). If the tendon is placed at eccentricity e from the center of gravity of the concrete, termed the cgc line, it creates a moment P_e, and the ensuing stresses at midspan become

$$f^t = -\frac{P}{A_c} + \frac{Pec}{I_g} - \frac{Mc}{I_g} \qquad (4)$$

$$f_b = -\frac{P}{A_c} - \frac{Pec}{I_g} + \frac{Mc}{I_g} \qquad (5)$$

Since the support section of a simply supported beam carries no moment from the external transverse load, high tensile fiber stresses at the top fibers are cause by the eccentric prestressing force. To limit such stresses, the eccentricity of the prestressing tendon profile, the cgs line, is made less at the support section than at the midspan section, or eliminated altogether, or else a negative eccentricity above the cgc line is used. The cgs line is the profile of the center of gravity of the prestressing tendon and the cgc line is the profile of the center of gravity of the concrete.

2.3. Prestressed concrete beam analysis: Basic Concept Method

In the basic concept method of designing prestressed concrete elements, the concrete fiber stresses are directly computed from the external forces applied to the concrete by longitudinal prestressing and the external transverse load. Equations 4 and 5 can be modified and simplified for use in calculating stresses at the initial prestressing

stage and at service load levels. If P_i is the initial prestressing force before stress losses, and P_e is the effective prestressing force after losses, then

$$\gamma = \frac{P_e}{P_i}$$

can be defined as the residual prestress factor. Substituting r^2 for I_g/A_c in Equations 4 and 5, where r is the radius of gyration of the gross section, the expressions for stress can be rewritten as follows:

a) Prestressing Force Only

$$f^t = -\frac{P_i}{A_c}\left(1 - \frac{ec_t}{r^2}\right) \qquad (6)$$

$$f_b = -\frac{P_i}{A_c}\left(1 - \frac{ec_b}{r^2}\right) \qquad (7)$$

where c_t and c_b are the distances from the center of gravity of the section (the cgc line) to the extreme top and bottom fibers, respectively.

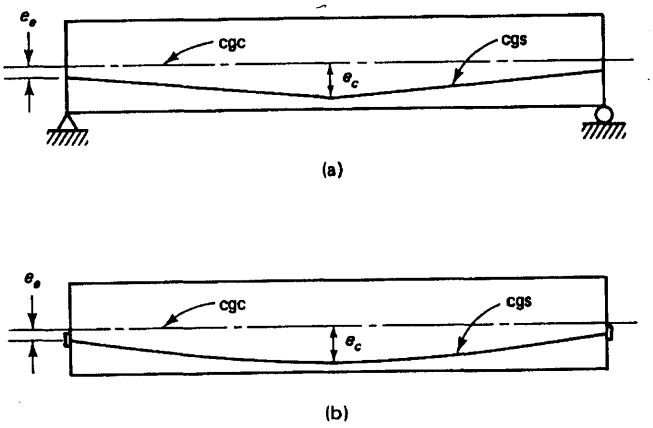

Figure 2.2

b) Prestressing Plus Self-weight

If the beam self-weight causes a moment M_D at the section under consideration, Equations 6 and 7 respectively become

$$f^t = -\frac{P_i}{A_c}\left(1 - \frac{ec_t}{r^2}\right) - \frac{M_D}{S^t} \qquad (8)$$

$$f_b = -\frac{P_i}{A_c}\left(1 - \frac{ec_b}{r^2}\right) + \frac{M_D}{S_b} \qquad (9)$$

Where S^t and S_b are the moduli of the sections for the top and bottom fibers, respectively.

The change in eccentricity from the midspan to the support section is obtained by raising the prestressing tendon either abruptly from the midspan to the support, a process called harping, or gradually in a parabolic form, a process called draping. Figure 2 shows a draped tendon usually used in post-tensioning.

Subsequent to erection and installation of the floor or deck, live loads act on the structure, causing a superimposed moment M_s. The full intensity of such loads normally occurs after the building is completed and some time-dependent losses in prestress have already taken place. Hence, the prestressing force used in the stress equations would have to be the effective prestressing force P_e. If the total moment due to gravity loads is M_T, then

$$M_T = M_D + M_{SD} + M_L \qquad (10)$$

where

M_D = moment due to self-weight

M_{SD} = Moment due to superimposed dead load, such as flooring

M_L = moment due to live load, including impact and seismic loads if any of the equations 8 and 9 become

$$f^t = -\frac{P_e}{A_c}\left(1-\frac{ec_t}{r^2}\right)-\frac{M_T}{S^t} \qquad (11)$$

$$f_b = -\frac{P_i}{A_c}\left(1-\frac{ec_b}{r^2}\right)+\frac{M_T}{S_b} \qquad (12)$$

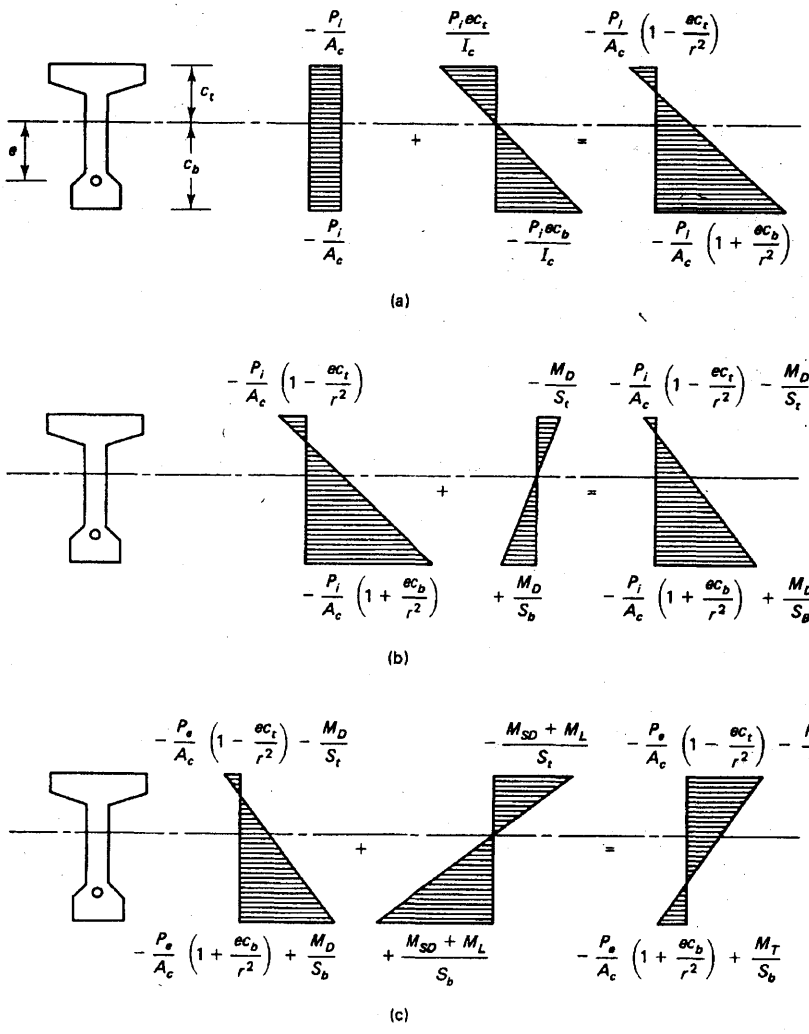

Figure 2.3

Some typical elastic concrete stress distributions at the critical section of a prestressed flanged section are shown in Figure 4. The tensile stress in the concrete in part c permitted at the extreme fibers of the section cannot exceed the maximum permissible in the code, e.g. $f_t = 6\sqrt{f'_c}$ in the ACI code. If it is exceeded, bonded non-prestressed reinforcement proportioned to resist the total tensile force has to be provided to control cracking at service loads.

2.4. Partial Loss of prestress

Prestressing force applied to the concrete elements undergoes a progressive process of reduction over a period of approximately five years. For this reason it is important to determine the level of the prestressing force at each loading stage, form the stage of transfer of the prestressing force to the concrete, to the various stages of prestressing available at service load, up to the ultimate.

The reduction in the prestressing force may happen immediately or time dependant. The first ones corresponds to an immediate elastic loss during the fabrication or construction process, including elastic shortening of the concrete, anchorage losses, and frictional losses. The second ones corresponds to the losses due to creep, shrinkage, and the ones originated by temperature effects and steel relaxation. All these losses may be determined at the service-load limit state of stress in the prestressed concrete element.

It is not feasible to determine with exactitude the magnitude of the mentioned above prestress losses, specially the time dependent ones. However, a very high degree of refinement of loss estimation is not desirable, because of the multiplicity of the many factors affecting the estimate.

For the case of post-tensioned members the total loss in prestressed can be calculated as follows:

$$\Delta f_{pT} = \Delta f_{pA} + \Delta f_{pF} + \Delta f_{pES} + \Delta f_{pR} + \Delta f_{pCR} + \Delta f_{pSH}$$

where Δf_{pES} is applicable only when tendons are jacked sequentially, and not simultaneously.

In the post-tensioned case, computation of relaxation loss starts between the transfer time $t_1 = t_{tr}$ and the end of the time interval t_2 under consideration. Hence

$$f_{pi} = f_{pi} - \Delta f_{pA} - \Delta f_{pF}$$

2.4.1. Elastic shortening of concrete (ES)

Concrete shortens when a prestressing force is applied. As the tendons that are bonded to the adjacent concrete simultaneously shorten, they lose part of the prestressing force that they carry.

The compressive force imposed on the beam by the tendon result in the longitudinal shortening of the beam. The unit shortening in concrete is $\varepsilon_{ES} = \Delta_{ES} / L$, so

$$\varepsilon_{ES} = \frac{f_c}{E_c} = \frac{P_i}{A_c E_c} \qquad (13)$$

Since the prestressing tendon suffers the same magnitude shortening,

$$\Delta f_{pES} = E_s \varepsilon_{ES} = \frac{E_s P_i}{A_c E_c} = \frac{nP_i}{A_c} = nf_{cs} \qquad (14)$$

$$f_{cs} = -\frac{P_i}{A_c} \qquad (15)$$

If the tendon has an eccentricity e at the beam midspan and the self-weight moment M_D is taken into account, the stress the concrete undergoes at the midspan section at the level of the prestressing steel becomes

$$f_{cs} = -\frac{P_i}{A_c}\left(1 + \frac{e^2}{r^2}\right) + \frac{M_D e}{I_c} \qquad (16)$$

where P_i has a lower value after transfer of prestress. The small reduction in the value of P_J to P_i occurs because the force in the prestressing steel immediately after transfer is less than the initial jacking prestress force P_J. However, since it is difficult to accurately determine the reduce value of P_i, and since observations indicate that the reduction is only a few percentage points, it is possible to use the initial valued of P_i before transfer in Equations 13 to 16, or reduce it by about 10 percent for refinement if desired.

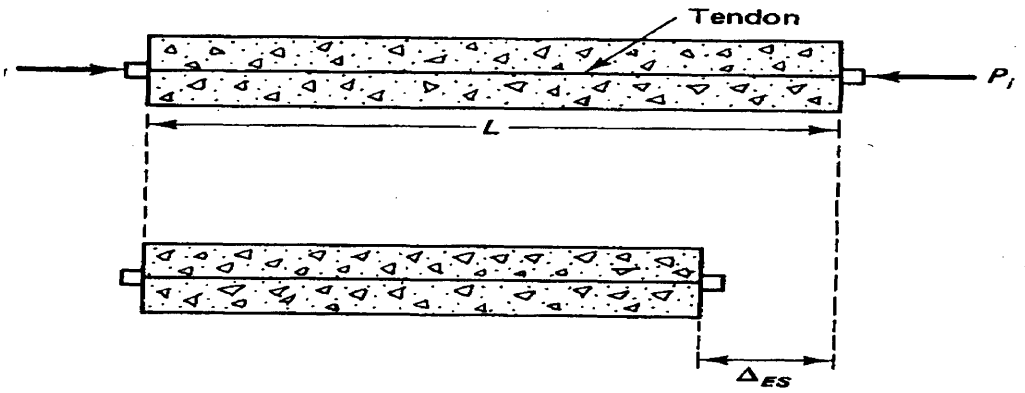

Figure 2.4

In post-tensioned beams , the elastic shortening loss varies from zero if all tendons are jacked simultaneously to half the value corresponding for the Δf_{pES} shortening if several sequential jacking steps are used, such as jacking two tendons at a time. IF *n* is the number of tendons or pairs of tendons sequentially tensioned, then

$$\Delta f_{pES} = \frac{1}{n}\sum_{j=1}^{n}(\Delta f_{pES})_j \qquad (17)$$

where *j* denotes the number of jacking operations. Note that the tendon that was tensioned last does not suffer any losses due to elastic shortening, while the tendon that was tensioned first suffers the maximum amount of loss.

2.4.2. Steel Stress relaxation (R)

Stress-relieved tendons suffer loss in the prestressing force due to constant elongation with time. The magnitude of the decrease in the prestress depends not only on the duration of the sustained prestressing force, but also on the ratio f_{pi}/f_{py} of the initial prestress to the yield strength of the reinforcement. Such a loss in stress is termed stress relaxation. The *ACI 318-89* Code limits the tensile stress in the prestressing tendons to the following:

a) For stresses due to the tendon jacking force, $f_{pJ} = 0.94\, f_{py}$, but not greater than the lesser of $0.80f_{py}$ and the maximum value recommended by the manufacturer of the tendons and anchorages.
b) Immediately after prestress transfer, $f_{pi} = o.82f_{py}$, but not greater than $0.74f_{pu}$.
c) In post-tensioned tendons, at the anchorages and couplers immediately after tendon anchorage the stress f_{pJ} at jacking should not exceed $0.80f_{pu}$.

The range of values of f_{py} is given by the following:

Prestressing bars: $f_{py} = 0.80 f_{pu}$

Stress-relieved tendons: $f_{py} = 0.85 f_{pu}$

Low-relaxation tendons: $f_{py} = 0.90 f_{pu}$

If f_{pR} is the remaining prestressing stress in the steel after relaxation, the following expression defines f_{pR} for stress relieved steel:

$$\frac{f_{pR}}{f_{pi}} = 1 - \left(\frac{\log t_2 - \log t_1}{10} \right) \left(\frac{f_{pi}}{f_{py}} - 0.55 \right) \tag{18}$$

2.4.3. Creep Loss (CR)

Experimental work over the past half century indicates that flow in materials occurs with time when load or stress exists. It consistson a lateral flow or deformation due to the longitudinal stress.

The deformation or strain resulting from this time dependent behavior is a function of the magnitude of the applied load, its duration, the properties of the concrete including its mix proportions, curing conditions, the age of the element at first loading, and environmental conditions. Since the stress-strain relationship due to creep is essentially linear, it is feasible to relate the creep strain ε_{cr} to the elastic strain ε_{EL} such that a creep coefficient C_u can be defined as

$$C_u = \frac{\varepsilon_{CR}}{\varepsilon_{EL}} \tag{19}$$

$$C_t = \frac{t^{0.60}}{10 + t^{0.60}} C_u \tag{20}$$

The value of C_u ranges between 2 and 4, with an average of *2.35* for ultimate creep. The loss in prestressed members due to creep can be defined for bonded members as

$$\Delta f_{pCR} = C_r \frac{E_{ps}}{E_c} f_{cs} \qquad (21)$$

where f_{cs} is the stress in the concrete at the level of the centroid of the prestressing tendon. In general, this loss is a function of the stress in the concrete at the section being analyzed. In post-tensioned, nonbonded members, the loss can be considered essentially uniform along the whole span. Hence, and average valued of the concrete stress f_{cs} between the anchorage points can be used for calculating the creep in post-tensioned members.

The *ACI-ASCE* Committee expression for evaluating creep loss has essentially the same format as equation 20

$$\Delta f_{pCR} = K_{CR} \frac{E_{pt}}{E_c} (\bar{f}_{cs} - \bar{f}_{csd}) \qquad (22)$$

or

$$\Delta f_{pCR} = nK_{CR} (\bar{f}_{cs} - \bar{f}_{csd}) \qquad (23)$$

where K_{CR} = *2.0* for pretensioned members

= *1.60* for post-tensioned members (both for normal concrete)

$\bar{f}$ = stress in concrete at level of steel cgs immediately after transfer

$\bar{f}_{csd}$ = stress in concrete at level of steel cgs due to all superimposed dead loads applied after prestressing is accomplished

n = modular ratio

2.4.4. Shrinkage Loss (SH)

As with concrete creep, the magnitude of concrete is affected by several factors. They include mix proportions, type of aggregate, type of cement, curing time, time between the end of external curing and the application of prestressing, size of the member, and the environmental conditions. Size and shape of the member also affect shrinkage. Approximately 80 percent of shrinkage takes place in the first year of life of the structure. The average value of ultimate shrinkage strain in both moistured and steam-cured concrete is given as *780x10-6 in./in.* in *ACI 209 R-92* Report. This average value is affected by the length of initial moist curing, ambient relative humidity, volume-surface ratio, temperature, and concrete composition. To take such effects into account, the average value of shrinkage strain should be multiplied by a correction factor γ_{sh} as follows

$$\varepsilon_{sh} = 780x10^{-6}\gamma_{sh} \qquad (24)$$

Components of γ_{sh} are factors for various environmental conditions.

The Prestressed Concrete Institute stipulates for standard conditions an average value for nominal ultimate shrinkage strain $(\varepsilon_{sh})_u = 820x10^{-6}$ *in./in. (mm/mm).* If ε_{sh} is the shrinkage strain after adjusting for relative humidity at volume-to-surface ratio *V/S*, the loss in prestressing in pretensioned members is

$$\Delta f_{pSH} = \varepsilon_{SH}\, xE_{ps} \qquad (25)$$

For post-tensioned members, the loss in prestressing due to shrinkage is somewhat less since some shrinkage has already taken place before post-tensioning. If the relative humidity is taken as a percent value and the *V/S* ratio effect is considered, the PCI general expression for loss in prestressing due to shrinkage becomes

$$\Delta f_{pSH} = 8.2x10^{-6} K_{SH} E_{ps} \left(1 - 0.06\frac{V}{S}\right)(100 - RH) \qquad (26)$$

where K_{SH} = *1.0* for pretensioned members. The *table 1* gives the values of K_{SH} for post-tensioned members.

time	1	3	5	7	10	20	30	60
K_{sh}	0.92	0.85	0.80	0.77	0.73	0.64	0.58	0.45

Table 1

Adjustment of shrinkage losses for standard conditions as a function of time *t* in days after seven days for moist curing and three days for steam curing can be obtained from the following expressions

a) Moist curing, after seven days

$$(\varepsilon_{sh})_t = \frac{t}{t+35}(\varepsilon_{sh})_u \qquad (27)$$

where $(\varepsilon_{sh})_u$ is the ultimate shrinkage strain, *t* – time in days after shrinkage is considered.

b) Steam curing, after one to three days

$$(\varepsilon_{sh})_t = \frac{t}{t+55}(\varepsilon_{sh})_u \qquad (28)$$

It should be noted that significant variations occur in the creep and shrinkage values due to variations in the properties of the constituent materials form the various sources, even if the products are plant-produced such as pretensioned beams. Hence

it is recommended that information for actual tests be obtained especially on manufactured products, large span-to-depth ratio cases and/or if loading is unusually heavy, like may be the present case of study.

2.5. Deflection calculations in prestressed concrete

Deflection and cracking behavior are very important factors in the design of prestressed concrete members. Prestressed concrete elements are typically more slender than their counterparts in reinforced concrete, and their behavior more affected by flexural cracking, makes it more critical to control their deflection and cracking. Before cracking, the deflections of prestressed-concrete beams can be predicted with greater precision than that of reinforced-concrete beams. Under working loads, prestressed-concrete beams do not crack; reinforced ones do.

For a typical beam, application of prestress force will produce upward camber. The effect of concrete shrinkage, creep, and steel relaxation is gradually to reduce the camber produced by the initial force as that force is diminished. However, the creep effect is twofold. Although it produces loss of prestress force, tending to reduce the camber, creep strains in the concrete usually increase the negative curvature associated with prestress and, hence, increase the camber. Either of these time-dependent effects may predominate, depending on the details of the design and the material properties.

Dead and live loads usually produce downward deflections that superimpose on the upward deflection due to prestress. In the case of sustained loads, these too are time-dependent because of concrete creep.

By prestressing, it is possible to control deflections to a remarkable degree. In fact, it is only through deflection control that the high span-to-depth ratios typical of

prestressed concrete can be achieved. A prestressed beam of a given cross section is considerably stiffer than a reinforced concrete beam of the same section, because cracking is reduced or eliminated by prestressing. Thus, all of nearly all of the cross section contributes to the moment of inertia and the flexural rigidity.

The primary design involves proportioning the structural member for the limit state of flexural stresses at service load and for limit states of failure in flexure, shear, and torsion, including anchorage development strength. Such a design can only become complete if the magnitudes of long-term deflection, camber (reverse deflection), and crack width are determined to be within allowable serviceability values.

As usually encountered for any concrete member, two difficulties still stand in the way when we wish to get an accurate prediction of the deflections. First, it is difficult to determine the value of E_c within an accuracy of 10% or even 20%. Besides, the value of E_c varies for different stress levels and changes with the age of concrete. The second difficulty lies in estimating the effect of creep on deflections. The value of creep coefficient as well as the duration and magnitude of the applied load cannot always be known in advance. However, for practical purposes, an accuracy of 10% or 20% is often sufficient, and that can be attained if all factors are carefully considered.

Deflections of prestressed beams differ from those of ordinary reinforced beams in the effect of prestress.

If the prestress force is accurately known, if the materials are stressed only within their elastic ranges, and if the concrete remains uncracked, then the calculation of deflection of a prestressed flexural member presents no special difficulty.

The difficulty of predicting very accurately the total long-term prestress losses makes it more difficult in partially prestressed concrete systems, where limited cracking is allowed through the use of additional nonprestressed reinforcement. Creep strain in

the concrete increases camber, as it causes a negative increase in curvature which is usually more dominant than the decrease produced by the decrease in prestress losses due to creep, shrinkage, and stress relaxation. A best estimate of camber increase should be based on accumulated experience, span-to-depth ratio code limitations, and a correct choice of the modulus E_x of the concrete. Calculation of the moment-curvature relationships at the major incremental stages of loading up to the limit state at failure would also assist in giving a more accurate evaluation of the stress-related load deflection of the structural element.

The cracking aspect of serviceability behavior in prestressed concrete is also critical. Allowance for limited cracking in "partial prestressing" through the additional use of nonprestressed steel is prevalent. Because of the high stress levels in the prestressing steel, corrosion due to cracking can become detrimental to the service life of the structure.

Partial prestressing consists on subjecting the beam to an intermediate solution between fully prestressed and reinforced concrete. Although full prestressing offers the possibility of complete elimination of cracks at full service load, it may at the same time produce members with objectionably large camber, or negative deflection, at more typical loads less than the full value. A smaller amount of prestress force may produce improved deflection characteristics at load stages of interest. While cracks will usually form in partially prestressed beams should the specified full service load be applied these cracks are small and will close completely when the load is reduced.

In addition to improved deflection characteristics, partial prestressing may result in significant economy by reducing the amount of prestressed reinforcement and by permitting the use of cross-section configurations with certain practical advantages compared with those required by full prestressing.

Even though the amount of prestress force may be reduced through use of partial prestressing, a beam must still have an adequate factor of safety against failure. This will often require the addition of ordinary reinforcing bars in the tension zone. Alternatives are to provide the total steel area needed for strength by high strength tendons, but to stress those tendons to less than their full permitted value, or to leave some of the strands unstressed.

2.5.1. Basic assumptions in deflection calculations:

Deflection calculations can be made either from the moment diagrams of the prestressing force and the external transverse loading, or form the moment-curvature relationships. In either case, the following basic assumptions have to be made:

1. The concrete gross cross-sectional area is accurate enough to compute the moment of inertia except when refined computations are necessary.
2. The modulus of concrete $E_c = 33w^{1.5}\sqrt{f'_c}$, where the value of f'_c corresponds to the cylinder compressive strength of concrete at the age at which E_c is to be evaluated.
3. The principle of superposition applies in calculating deflections due to transverse load and camber due to prestressing.
4. All computations of deflection can be based on the center of gravity of the prestressing strands (cgs), where the strands are treated as a single tendon.
5. Deflections due to shear deformations are disregarded.
6. Sections can be treated as totally elastic up to the decompression load. Thereafter the cracked moment of inertia I_{cr} can give a more accurate determination of deflection and camber.

2.5.2. Short-term (instantaneous) deflection of cracked members

Short-term deflections in prestressed concrete members are calculated on the assumption that the sections are homogeneous, isotropic, and elastic. Such an assumption is an approximation of actual behavior, particularly that the modulus Ec of concrete varies with the age of the concrete and the moment of inertia varies with the stage of loading, i.e., whether the section is uncracked or cracked.

Ideally, the load-deflection relationship is trilinear. The three regions prior to rupture are:

Region I. Precracking stage, where a structural member is crack fee.
Region II. Postcracking stage, where the structural member develops acceptable controlled cracking in both distribution and width.
Region III. Postserviceability cracking stage, where the stress in the tensile reinforcement reaches the limit state of yielding.

At the precracking region the segment of the load-deflection curve is essentially a straight line defining full elastic behavior. The maximum tensile stress in the beam in this region is less than its tensile strength in flexure, i.e., it is less than the modulus of rupture f_r of concrete. The flexural stiffness *EI* of the beam can be estimated using Young's modulus E_c of concrete and the moment of inertia of the uncracked concrete cross section.

The value of E_c can be estimated using the ACI empirical expression

$$E_c = 33w^{1.5}\sqrt{f'_c} \tag{29}$$

or

$$E_c = 57{,}000\sqrt{f'_c} \quad \text{for normal-weight concrete} \tag{30}$$

The precracking region stops at the initiation of the first flexural crack, when the concrete stress reaches its modulus of rupture strength f_r. Similarly to the direct tensile splitting strength, the modulus of rupture of concrete is proportional to the square root of its compressive strength. For design purposes, the value of the modulus of rupture for concrete may be taken as

$$f_r = 7.5\lambda\sqrt{f'_c} \tag{31}$$

where $\lambda = 1.0$ for normal-weight concrete. If all-lightweight concrete is used, then $\lambda = 0.75$, and if sand-lightweight concrete is used, $\lambda = 0.85$.

If one equates the modulus of rupture f_r to the stress produced by the cracking moment M_{cr} (decompression moment), then

$$f_b = f_r = -\frac{P_e}{A_c}\left(1 + \frac{ec_b}{r^2}\right) + \frac{M_{cr}}{S_b} \tag{32}$$

Where subscript b stands for the bottom fibers at midspan of a simply supported beam. If the distance of the extreme tension fibers of concrete from the center of gravity of the concrete section is y_t, then the cracking moment is given by

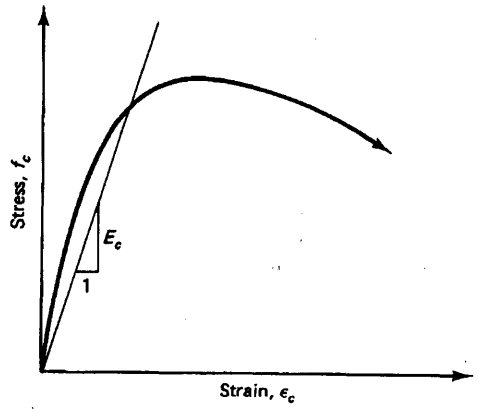

Figure 2.6

$$M_{cr} = \frac{I_g}{y_t}\left[\frac{P_e}{A_c}\left(1+\frac{ec_b}{r^2}\right)+7.5\lambda\sqrt{f'_c}\right] \quad (33)$$

$$M_{cr} = S_b\left[7.5\lambda\sqrt{f'_c}+\frac{P_e}{A_c}\left(1+\frac{ec_b}{r^2}\right)\right] \quad (34)$$

when S_b = section modulus at the bottom fibers. More conservatively, from the equation shown below, the cracking moment due to that portion of the applied live load that causes cracking is

$$M_{cr} = S_b\left[7.5\lambda\sqrt{f'_c}+f_{ce}-f_d\right] \quad (35)$$

where

f_{ce} = compressive stress at the center of gravity of concrete section due to effective prestress only after losses when tensile stress is cause by applied external load

f_d = concrete stress at extreme tensile fibers due to unfactored dead load when tensile stresses and cracking are caused by the external load.

Equation 35 can be transformed to the PCI format giving identical results:

$$\frac{M_{cr}}{M_a} = 1-\left(\frac{f_{tl}-f_r}{f_L}\right) \quad (36)$$

where

M_a = maximum service unfactored live load moment

f_{tl} = final calculated total service load concrete stress in the member

f_r = modulus of rupture

f_L = service live load concrete stress in the member

2.5.2.1. Cracked Sections: Effective-moment-of-inertia computation method.

As the prestressed element is overloaded, or in the case of partial prestressing where limited controlled cracking is allowed, the use of the gross moment of inertia I_g underestimates the camber or deflection of the prestressed beam. Theoretically, the cracked moment of inertia I_{cr} should be used foe the section across which the cracks develop while the gross moment of inertia I_g should be used for the beam sections between the cracks.

However, such refinement in the numerical summation of the deflection increases along the beam span is sometimes unwarranted because of the accuracy difficulty of deflection evaluation. Consequently, an effective moment of inertia I_e can be used as an average value along the span of a simply supported bonded tendon beam. According to this method,

$$I_e = I_{cr} + \left(\frac{M_{cr}}{M_a}\right)^3 \left(I_g - I_{cr}\right) \leq I_g \qquad (37)$$

$$I_e = \left(\frac{M_{cr}}{M_a}\right)^3 I_g + \left[1 - \left(\frac{M_{cr}}{M_a}\right)^3\right] I_{cr} \leq I_g \qquad (38)$$

The ratio (M_{cr}/M_a) from Equation 36 can be substituted into Equation 37 and b to get the effective moment of inertia

$$\frac{M_{cr}}{M_a} = 1 - \left(\frac{f_{tl} - f_r}{f_L}\right) \qquad (39)$$

where

I_{cr} = moment of inertia of the cracked section, form Equation 40 to follow

I_g = gross moment of inertia

Note that both M_{cr} and M_a are the unfactored moments due to live load only such that M_{cr} is taken as that portion of the live load moment which causes cracking. The effective moment of inertia I_e in Equations 37 and b thus depends on the maximum moment M_a along the span in relation to the cracking moment capacity M_{cr} of the section.

The cracking moment of inertia can be calculated by the PCI approach.

For fully prestressed members

$$I_{cr} = n_p A_{ps} d_p^2 (1 - 1.6\sqrt{n_p \rho_p}) \tag{40}$$

For partial prestressing

$$I_{cr} = (n_p A_{ps} d_p^2 + n_x A_s d^2)(1 - 1.6\sqrt{n_p \rho_p + n_s \rho}) \tag{41}$$

In the case of uncracked continuous beams with both ends continuous,

$$Avg.I_e = 0.70 I_m + 0.15(I_{e1} + I_{e2}) \tag{42}$$

and for continuous uncracked beams with one end continuous,

$$Avg.I_e = 0.85 I_m + 0.15(I_{cont.end}) \tag{43}$$

where I_m is midspan section moment of inertia and I_{e1} and I_{e2} are the end-section moments of inertia.

2.5.3. Long-term effects on deflection and camber: PCI Multipliers Method

The ACI Code provides the following equation for estimating the time-dependent factor for deflection of nonprestressed concrete members:

$$\lambda = \frac{\xi}{1+50\rho'} \qquad (44)$$

where

ξ = time-dependent factor for sustained load

ρ' = compressive reinforcement ratio

λ = multiplier for additional log-term deflection

In a similar manner, the PCI multipliers method provides a multiplier C_t which takes account of long-term effects in prestressed concrete members. C_t differs from λ in Equation 44, because the determination of long-term cambers and deflections in prestressed members is more complex due to the following factors:

1. The log-term effect of the prestressing force and the prestress losses.
2. The increase in strength of the concrete after release of prestress due to losses.
3. The camber and deflection effect during erection.

Because of these factors, Equation 44 cannot be readily used.

From tabuled it can provided reasonable multipliers of immediate deflection and camber are separated in order to take into account the effects of loss of prestress, which only apply to the upward component.

Shaikh and Branson propose that substantial reduction can be achieved in long-term camber by the addition of nonprestressed steel. In that case, a reduced multiplier C_2 can be used given by

$$C_2 = \frac{C_1 + A_s / A_{ps}}{1 + A_s / A_{ps}} \qquad (45)$$

where

C_1 = multiplier form Table 7.1

A_s = area of nonprestressed reinforcement

A_{ps} = area of prestressed strands

2.6. Indeterminate prestressed concrete structures: Continuous beams

Prestressed concrete has been largely used for the design of continuous multiple spans bridges in the past. One of the main reasons why it may be chosen despite single span is because there is a reduction of moments and stresses at midspans through the design of continuous systems resulting on shallower members. This members are stiffer than simply supported members of equal span and of comparable loading and are of lesser deflection.

Therefore, lighter structures will require smaller foundations both leading to a reduction in the cost of materials and construction. Moreover, it usually improves the resistance to longitudinal and lateral loads. As a result of this, the span-to-depth ratio is also improved, depending on the type of continuous system being considered. For continuous flat plates, a ratio of 40 to 45 is reasonable and for box girders this ratio can be 25 to 30.

Another advantage of continuous systems is the elimination of anchorages at intermediate supports through continuous post-tensioning over several spans, thereby reducing further the cost of materials and labor.

Continuous prestressed concrete is widely for the construction of long-span prestressed concrete bridges, particularly situ-cast post-tensioned spans. Cantilevered box girder bridges, widely used in Europe as segmental bridges, are increasingly being used in the United States.

The success of prestressed concrete construction is in an important part due to the economy of using precast elements, with the associated high quality control during fabrication. This desirable feature has been widely achieved by imposing continuity on the precast elements through placement of situ-cast reinforced concrete at the intermediate supports. The situ-cast concrete tends to resist the superimposed dead load and the live load that act on the spans after the concrete hardens.

However, there are several disadvantages of using continuity in prestressing and that must be taken to account for through appropriate design and construction of the final system:

1. Higher frictional losses due to the larger number of bends and longer tendons.
2. Concurrence of moment and shear at the support sections, which reduces the moment strength of those sections.
3. Excessive lateral forces and moments in the supporting columns, particularly if the y are rigidly connected to the beams. These forces are caused by the elastic shortening of the long-span beams under prestress.
4. Effects of higher secondary stresses due to shrinkage, creep temperature variations, and settlement of the supports.

5. Secondary moments due to induced reactions at the supporting columns caused by the prestressing force.
6. Possible serious reversal of moments due to alternate loading of spans.
7. Moment values at the interior supports that require additional reinforcement at these supports, which might otherwise no be needed in simply supported beams.

The construction system used, the length of the adjacent spans, and the engineering judgment along with the ingenuity of the design engineer determine the type of layout and method of framing to be used for achieving continuity. There are two categories of continuity in beams:

The monolithic continuity, where all the tendons are generally continuous throughout all or most of the spans and all tendons are prestressed at the site. Such prestressing is accomplished by pot-tensioning.

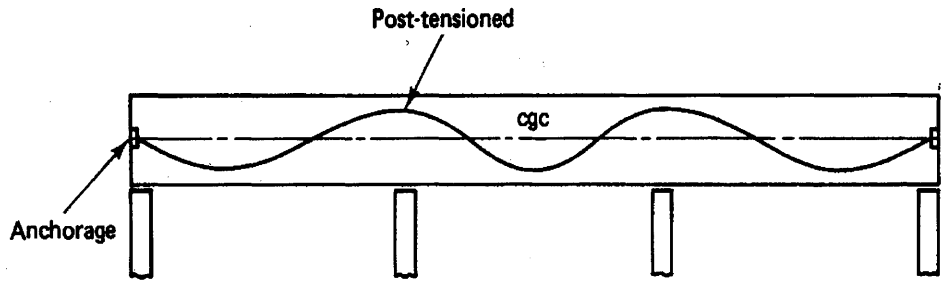

Figure 2.7a

Nonmonolithic continuity, where precast elements are used as simple beams on which continuity is imposed at the support sections through situ-cast reinforced

concrete which provides the desired level of continuity to resist the superimposed dead load and live load from the train after the concrete hardens.

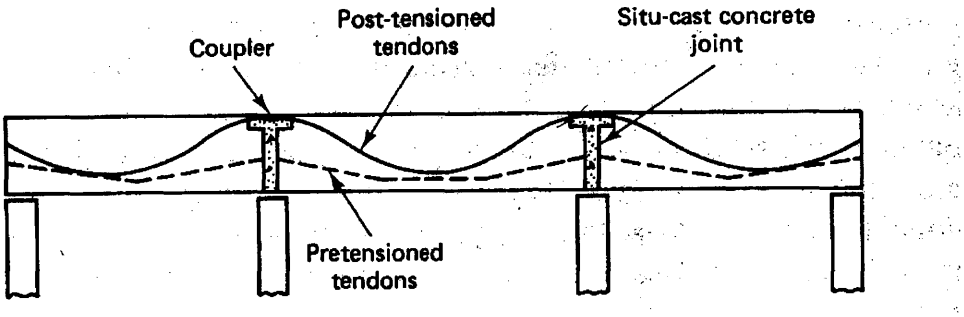

Figure 2.7b

3. Dynamic effects on structures derived from High-Velocity.

3.1. Rail bridge structural dynamics evolution.

The discipline of railway bridge dynamics has a rich history and great attention has been paid to the study of bridge dynamics all over the world. During the construction of the first railways in England in the first half of the 19th century, the engineers were split into two groups. One believed that the passage of a railway locomotive along the bridge would generate enough time to become deformed during the engine passage. For this reason, this very early period gave rise to the first experiments an to the first theoretical studies which suggested that the actual effect of a moving railway locomotive on the bridge would lie somewhere between those two extreme opinions mentioned above Since that time the dynamics of railway bridges has received consistent attention in most technically developed countries all over the world.

Between the two World Wars the dynamics of railway bridges was given greatest attention in the former USSR and in Great Britain. It was in this period of time when the two fundamental problems of motion of a constant and of an harmonically variable force along a beam were solved as well as the effects of steam railway locomotives on the statically indeterminate continuous, frame and arch railway bridges. For decades, many schools all over the world focus on the study of this discipline both theoretically and experimentally.

3.2. Dynamic Analysis

The dynamics of railway bridges is concerned with the study of deflections and stresses in railway bridges. The loads that participate in this scientific discipline are represented by the moving wheel and axle forces, by means of which railway vehicles transmit their load and inertia actions to railway bridges.

There are numerous parameters which may influence the magnitude of dynamic strains and stresses. The most important parameters influencing the dynamic stresses for this structures are the frequency characteristics of bridge structures (length, mass, and rigidity of individual members), the frequency characteristic of vehicles, the damping in bridges and in vehicles, the velocity of vehicle movement, the track irregularities, as well as others.

The vehicles affect the bridges not only by vertical forces, but also by movements which generate longitudinal and transverse horizontal forces. This effects results in an increase or decrease of bridge deformations comparing to the ones from the static loading effects. In engineering design practice the procedure is to consider a static effect multiplier factor which states how many times it has to be increased in order to cover the additional dynamic loads. This factor is very simple and does not take into account most of the parameters which influence the dynamic behavior of the structure. However, the factor is accurate enough as for ensuring the safety and reliability of this types of bridges.

Other factor to be taken into account is the fatigue of the structure. Because of the large number of vibration effects that a railway bridge may be subjected to during its life-cycle this may be a serious problem. A new approach may be followed which assumes that the magnitude and number of stress cycles generated in the bridge by the passage of all trains during its service life. Although this approach is closer to reality it will not be considered for the present study.

3.2.1. Deterministic vibration

The response of a railway bridge to the passage of a vehicle manifests itself as vibration. By deterministic vibration we understand the motion which can be predicted at all times. The basic model from the field of vibrations is a system with one degree of

freedom whose motion is described, according to Newton's second law and D'Alembert's principle, by the differential equation

$$m\frac{d^2v(t)}{dt^2}+b\frac{dv(t)}{dt}+kv(t)=F(t) \qquad (46)$$

where

v(t) = displacement of body of mass m at time t

m = lumped mass of the system

b = 2mωb damping force at unit velocity

k = stiffness or rigidity of the spring, assumed constant

F(t) = external force dependent on time t

The fundamental concepts in the field of vibrations are the natural circular frequency of the system as (Equation 46).

$$\omega_o=\left(\frac{k}{m}\right)^{1/2} \qquad (47)$$

the circular frequency of damped vibrations with subcritical damping

$$\omega_d=\omega_o^2-\omega_b^2 \qquad (48)$$

the natural frequencies of undamped or damped vibrations derived from it

$$f_o=\frac{\omega_o}{2\pi} \qquad (49)$$

$$f_d=\frac{\omega_d}{2\pi} \qquad (50)$$

respectively, and the period of natural vibrations

$$T_o = \frac{1}{f_o} \tag{51}$$

$$T_d = \frac{1}{f_d} \tag{52}$$

respectively, this being the shortest time after which the vibration repeats.

The damping of the system, as shown in equation 46, is characterized most frequently by the logarithmic decrement of damping, ξ, which is defined as the natural logarithm of the ratio of any two successive amplitudes of like sign after time T_d. In the case of damping proportional to vibration velocity, this ratio is constant. In practice, it is often determined on the basis of *n* successive vibrations.

$$\xi = \frac{1}{n} \ln \frac{s_o}{s_n} \tag{53}$$

where s_n is the amplitude after the nth cycle as shown in figure 3.1.

The relation of the logarithmic decrement of damping to the constant b or ωb in equation (46) is

$$\xi = \frac{\omega_b}{f_d} = \frac{b}{2mf_d} \tag{54}$$

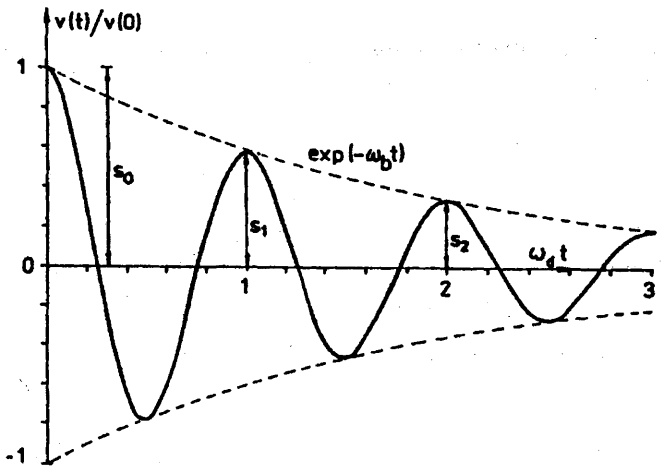

Figure 3.1

3.2.1.1. Dynamic coefficient

The dynamic coefficient, dynamic impact factor, dynamic magnification or dynamic amplification is usually defined as a dimensionless ration of the maximum dynamic displacement to the static displacement. In the simplest case, described by equation 46, it can be obtained as follows:

Analysis of the forced vibration of a system with one degree of freedom requires the solution of equation (1.1) under the action of a force

$$F(t) = F \sin \omega t \qquad (55)$$

At $t \to \infty$, the sustained vibration takes the form of

$$v(t) = A \sin \omega t + B \cos \omega t \qquad (56)$$

After the substitution of equations (55) and (56) in equation (46) and a comparison of coefficients of the individual terms we obtain the following expressions for the constants A and B:

$$A = \frac{F(\omega_o^2 - \omega^2)}{m[(\omega_o^2 - \omega^2)^2 + 4\omega^2\omega_b^2]}, \tag{57}$$

$$B = \frac{-2F\omega\omega_b}{m[(\omega_o^2 - \omega^2)^2 + 4\omega^2\omega_b^2]}, \tag{58}$$

The maximum amplitude of forced stationary vibrations is the vector sum of A and B, so

$$s_o = (A^2 + B^2)^{1/2} = \frac{F}{m}\left[(\omega_o^2 - \omega^2)^2 + 4\omega^2\omega_b^2\right]^{1/2} \tag{59}$$

The static displacement of a mass on the spring of stiffness k subjected to the force F, according to the definition of the spring stiffness (equation (47), is

$$v_s = \frac{F}{k} = \frac{F}{m\omega_o^2} \tag{60}$$

The dynamic coefficient for the simplest case of forced vibration of a system with one degree of freedom is the defined as the ratio of the maximum dynamic displacement (59) and the static displacement (60)

$$\delta = \frac{s_o}{v_{st}} = \left[(1 - \omega^2/\omega_o^2)^2 + \frac{4\omega^2\omega_b^2}{\omega_0^4}\right]^{-1/2} \tag{61}$$

and depends, consequently, on the ratio ω/ω_o and on $\beta = \omega_b/\omega_o$. The function (61) is represented graphically by the resonance curve in Figure 3.2.

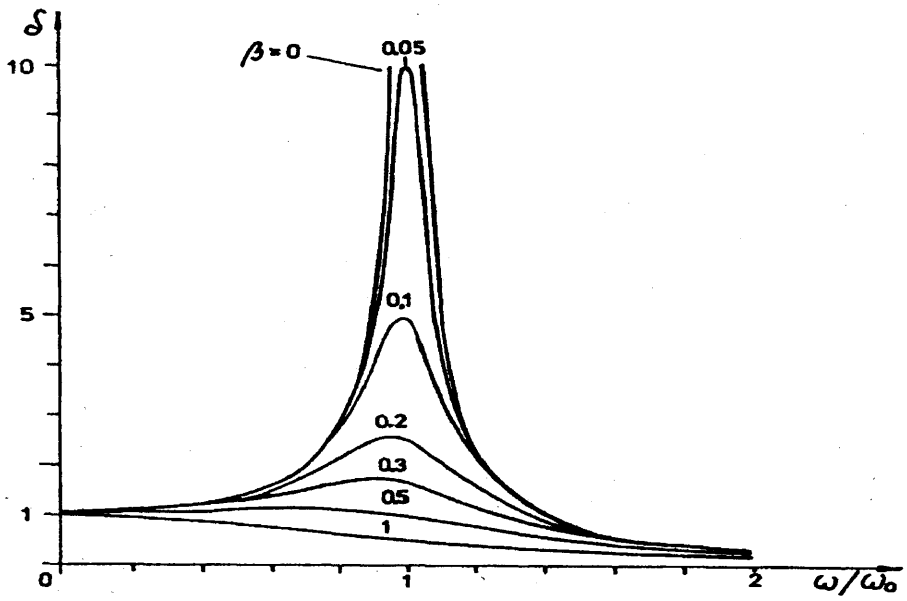

Figure 3.2

The maximum dynamic coefficient may be calculated from the condition that the expression $(1-\omega^2/\omega_0^2)+4\omega^2\omega^2/\omega_o^4$ (the denominator in equation (61) attains its minimum value. When derivative of this expression is made equal to zero the maximum dynamic coefficient is obtained when

$$\omega^2 = \omega_o^2 - 2\omega_b^2 \qquad (62)$$

This means that for small damping the highest effects arise when the frequency ω is approximately the natural frequency ω_o; that is

$$\omega = \omega_o \qquad (63)$$

This frequency produces strong (resonance) vibrations of the system.

If we substitute the excitation frequency (62) into equation (61), we obtain the maximum values of the dynamic coefficient (see also equations (54) and (55).

$$\delta_{\max} = \frac{\omega_o^2}{2\omega_b\omega_d} = \frac{\omega_o}{2\omega_b} = \frac{1}{2\beta} = \frac{\pi}{\xi} \qquad (64)$$

Equation (64) shows that maximum dynamic effect in resonance conditions depends chiefly on the damping characteristics of the system (it is indirectly proportional to the logarithmic decrement of damping).

3.2.2. Theoretical Bridge models

Railway bridges are generally long structures which is reflected also in the theoretical models used in their analysis. In principle, theoretical models of railway bridges are of two types: those with continuously distributed mass and those with mass concentrated in material points (lumped masses), or their combinations. The choice of an adequate model depends on the particular case and on the purpose of the analysis.

3.2.3. Beams

The railway bridge model most frequently used is a beam which models well and simply the linear character of the structure which has small transverse dimension when compared with its length.

3.2.4. Mass Beams

If the mass of the bridge structure is comparable with or considerably higher than the mass of the vehicles, it cannot be neglected. This is the case for medium and large

span bridges. In this way the mass beam is necessary which is used most frequently of theoretical idealization. The equation of motion of the beam expresses the equilibrium of forces per unit length:

$$EI\frac{\partial^4 v(x,t)}{\partial x^4} + \mu\frac{\partial^2 v(x,t)}{\partial t^2} + 2\mu\omega_\beta\frac{\partial v(x,t)}{\partial t} = f(x,t) \qquad (65)$$

Where $v(x,t)$ - vertical deflection of the beam at the point x and at time t,

E - modulus of elasticity of the beam,

I - moment of inertia of beam cross section,

μ - mass per unit length of the beam,

ω_b - circular frequency of viscous damping,

$f(x,t)$ -vertical deflection of the beam at the point x and at time t,

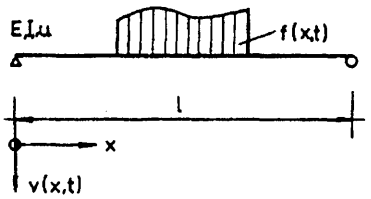

Figure 3.3

Differential equation (65) was derived by Bernoully and Euler assuming the theory of small deformations, the validity of Hooke's law, Navier's hypothesis and the Saint-Venant principle. Equation (65) assumes constant cross section and mass per unit length of the beam and the damping according to the Kelvin_Voigt model is considered proportional to the velocity of vibration.

Apart from the differential equation (65) the behavior of the beam can also be described by the following integral-differential equation

$$v(s,t) = \int_0^t G(x,s)\left[f(s,t) - \mu \frac{\partial^2 v(s,t)}{\partial t^2} - 2\mu\omega_b \frac{\partial v(s,t)}{\partial t} \right] ds \qquad (66)$$

Which follows from the theory of influence lines. In equation (66):

$G(x,s)$ - influence function of the beam also called Green's function. It is the deflection of the beam at point x due to a unit force applied at point s,

l - span of the beam.

Both methods, that using equation (65) and that using equation (66), are equivalent.

A current method of analysis is that using equation (65) which is applied in all analytical and numerical methods of applied mathematics. Equation (66) provides some advantages in those cases where the influence function *G(x,s)* is known, e.g. from the structural analysis. The advantage of the second method is that the theory of integral equations of Fredholm type makes it sometimes possible to estimate the error by considering a finite number of successive approximations.

The idealization of railway bridges neglecting the mass of the structure is not used, because railway bridges must always be sufficiently stiff.

The theoretical model of suspension bridges can be derived from the equation

$$EI \frac{\partial^4 v(x,t)}{\partial x^4} - N \frac{\partial^2 v(x,t)}{\partial x^2} + \mu \frac{\partial^2 v(x,t)}{\partial t^2} + 2\mu\omega_b \frac{\partial v(x,t)}{\partial t} = f(x,t) \qquad (67)$$

Which is a combination of equation (65) and the equation of considering the beam stiffness negligibly small, obtaining a string, whose carrying capacity is provided by the horizontal force *N* stretching the string.

3.2.5. Continuous beams

In a continuous the continuity above intermediate supports is ensured by special conditions which form the core of the individual methods of analysis of continuous beams in structural mechanics, such as the slope-deflection method, the statical method, the method of initial parameters, the three-moment equation, the five moment equation, and others.

Figure 3.4

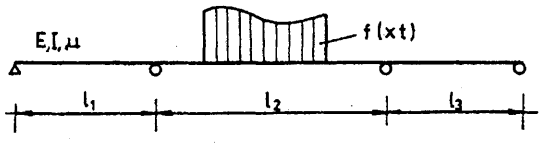

Analogous procedures are applied in special cases of continuous beams, such as structures with suspended spans, cantilever ends, and so on.

3.2.6. Boundary and initial conditions

The differential equations (65), (66) and (67) necessitate boundary conditions expressing mathematically the bearing of beam ends on supports according to fig. 3.5. We can discern the following types of bearings of beams:

Hinged bearing (Fig. 3.5a); this has zero deflection and bending moment at the point x = 0 (or at the point $x = L$), so

$$v(x,t) = 0 \qquad \text{and} \qquad \frac{\partial^2 v(x,t)}{\partial x^2} = 0 \tag{68}$$

The hinged bearing (Fig. 3b); is described by the same equations as equation (68).

A clamped beam end (Fig. 3.5c) has zero deflection and rotation, so

$$v(x,t) = 0 \quad \text{and} \quad \frac{\partial v(x,t)}{\partial x} = 0 \tag{69}$$

The free end (Fig. 3.5d) has a zero bending moment and shear force, so

$$\frac{\partial^2 v(x,t)}{\partial x^2} = 0 \quad \text{and} \quad \frac{\partial^3 v(x,t)}{\partial x^3} = 0 \tag{70}$$

Continuous beams must obey conditions above the supports, i.e. the conditions of deflection, rotation, bending moment and the shear force limiting from the right and from the left had sides.

The geometric conditions for x = 0 and x = l

$$v(x,t) \quad , \quad \frac{\partial v(x,t)}{\partial x} \tag{71}$$

And the dynamic conditions

$$\frac{\partial^2 v(x,t)}{\partial x^2} \quad , \quad \frac{\partial^3 v(x,t)}{\partial x^3} \tag{72}$$

Are generally different.

In the integral-differential equation (66) the boundary conditions are already included in the influence functions $G(x,s)$ which must satisfy them.

The initial conditions express the initial deformation and velocity of the structure at the time $t = 0$ from which we begin the analysis. Naturally, they can also be functions of spatial coordinates, such as for $t = 0$.

$$v(x,t) = g_1(x) \quad \text{and} \quad \frac{\partial v(x,t)}{\partial t} = g_2(x) \tag{73}$$

3.2.7. Prestressed concrete bridges

In prestressed concrete bridges, there are two principal cases: the prestressing tendons are either perfectly grouted or are entirely free.

In prestressed concrete railway bridges the reinforcement is bounded with concrete along the whole tendon length both in pre-tensioned and in post-tensioned beams. Thus the state approaches the first case. In this case the prestress in the tendons has no influence on the potential energy of the beam and, therefore, it does not cause any changes in its natural frequencies. The overall forces applied to the element of length do not vary, because the prestressing force is in equilibrium with the forces compressing concrete. Therefore, in the case of grouted tendons, we proceed with the dynamic analysis of the beam according to equation (65) as if the beam were not subjected to an axial force. We include the concrete cross section in full and the ideal cross section of reinforcement into the cross section area of the beam and prestress. This procedure is applied, whether the beam is pre-tensioned or post-tensioned.

In the second case, when the beam is exposed to constant compression N at its ends only according to Fig. 3.16 the equation 65 is applied. The natural frequencies of such a beam are influenced by the axial force. However, the tendons of such bridges would have to be free along their whole length, i.e. not embedded in concrete, situated on the neutral axis of the beam, and their stresses should not vary in the course of vehicle passage.

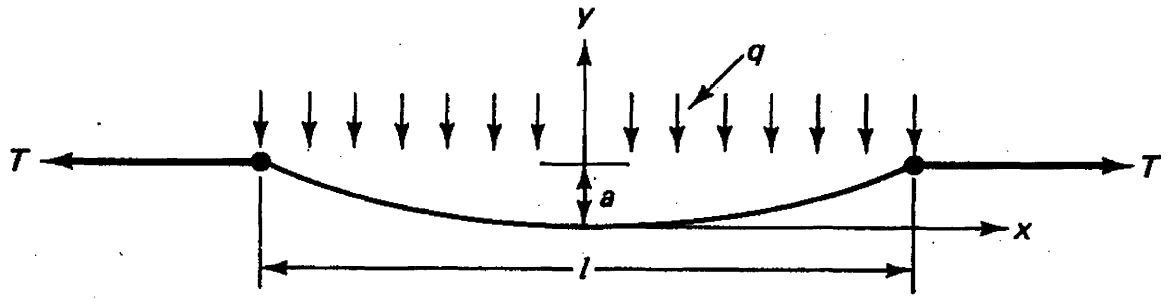

Figure 3.6

3.2.8. Influence of vehicle speed on dynamic stresses of bridges

Vehicle speed is the most important parameter influencing the dynamic stresses in railway bridges. In general, the dynamic stresses in bridges increase with increasing speed. We will show, that they depend also on the bridge and vehicle dynamic system, track irregularities and other parameters.

Considering the general tendency to increasing speed, the dynamic stresses in bridges at higher vehicle speeds have been gven considerable attention. For example, the Office for Research and Experiments (ORE) of the International Union of Railways (UIC) concentrated several research programs in this field to elucidate the problem with respect to stresses, fatigue, noise and the effect on man. Also Japanese National

Railways tested their bridges at height vehicle speeds. Up-to-date field measurements have verified dynamic stresses in railway bridges at vehicle speeds up to 250 km/h

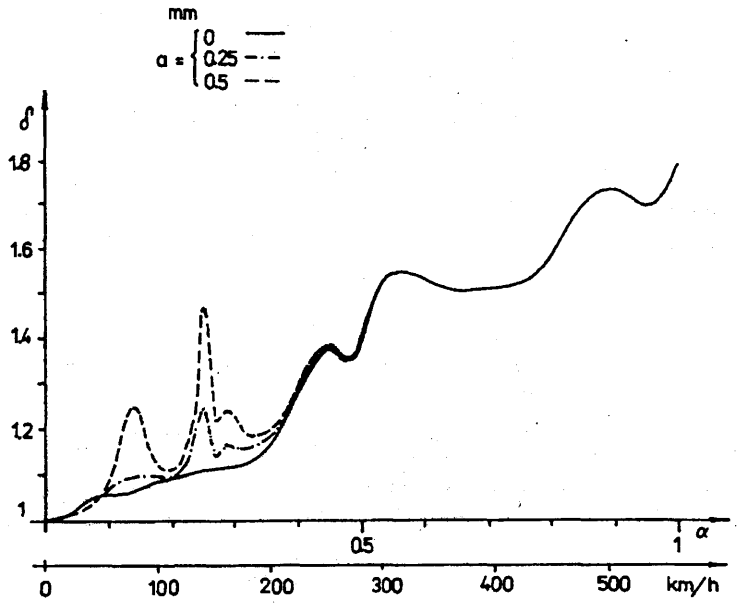

Figure 3.7

Theoretical analyses consider constant speed of motion of vehicles along the bridge, which is usually so in practice. The actual speed depends on the horizontal and vertical track alignment on the bridge. Even in the cases where the bridges are in poor condition or are temporary the speed remains constant even thought it is reduced.

However, in those cases when the vehicles or the train start or brake on bridges the speed is variable.

A constant velocity of motion is the simplest, i.e., the motion of a concentrated force F along a simply supported beam at constant velocity.

3.2.8.1. Motion based design.

3.2.8.1.1. Dynamic Considerations.

It is the main purpose of this paper to perform a dynamic analysis of a railway track under moving vibratory masses will as well be studied in this thesis. In such problems the critical velocity is an important parameter. This is influenced by the dynamical characteristics of the moving load. The track is modeled as an infinitely long Euler-Bernoulli beam on Winkler foundation. A novel approach to obtain the steady-state response of the track subjected to N equispaced in-phase oscillatory moving masses. Effects of mass spacing and number of masses on the resonant frequency and critical velocity will be studied. Track response due to a moving oscillatory line mass will also presented.

The loads are represented by the moving wheel and axle forces, by means of which the railway vehicles transmit their load and inertia actions to the bridges. Thus the dynamics of railway bridges involves the response of bridges to the movement of vehicles and to the influence of a number of parameters which increase dynamic strains or stresses. The most important parameters influencing the dynamic stresses in railway bridges are: the frequency characteristics of bridge structures (i.e. the length, mass, and rigidity of individual members), the frequency characteristic of vehicles (i.e. the sprung and unsprung masses, the stiffness of springs), the damping in bridges and in vehicles, the velocity of the vehicle movement, the track irregularities, and so on.

3.2.8.1.2. Critical speed.

It will be discussed in this paper, as mentioned before, the critical speed, the 'bow-wave' effect and how it is influenced by soil stiffness. In order to reach the centers of major conurbation, modern high-speed rail lines are increasingly utilizing marginal land avoiding previously built housing areas. This land often has low soil stiffness. The critical speed of waves across such soils can approach the speed of modern high-speed

trains. The large deflections caused can increase environmental noise and the track maintenance required and decrease ride quality. This paper discusses how.

The modeling of possible remedies to the problem will be discussed. A convolution technique is used to model axles travelling at different speeds and the effects of multiple axles. The resulting displacements are highly dependent on the amount of damping introduced into the system modeled. In-situ testing, laboratory testing and finite element modeling are compared and are shown to provide consistent results. The conclusion is that a powerful analytical tool for the prediction of the 'bow-wave' effect has been devised.

3.2.9. Influence of fatigue on dynamic stresses of bridges

The vehicles affect the bridges not only by vertical forces, but also by movements which generate longitudinal and transverse horizontal forces. This results in an increase or decrease of bridge deformations when compared to that due to static forces. In design practice, these effects are described by the dynamic coefficient (or dynamic impact factor) which, however, only states how many times the static effects must be multiplied in order to cover the additional dynamic loads.

The fatigue assessment of bridges has resulted in the derivation of a new approach. This assumes the magnitude and number of stress cycles generated in the bridge by the passage of all trains during its service life. This approach, which is closer to reality, has yielded valuable data for the fatigue assessment of bridges, for the estimation of their fatigue life and for the determination of inspection intervals.

3.2.10. Influence of thermal contribution on dynamic stresses of bridges

Therefore, it will not be necessary to go over the problem of thermal interaction. Although the temperature changes also depend on time the thermal effects do not generate any vibration in bridges.

3.2.11. Influence of soil contribution on dynamic stresses of bridges

We have to take into account that the modern high-speed rail lines are being built increasingly on marginal land, in order to reach city centers while avoiding housing areas. Often this land is composed of soft alluvial soils, which exhibit a low resilient modulus. The measurement, prediction, modeling, and implications of resilient modulus values for such subgrades are being discussed. Measurement must consider the use of repeated, load triaxial testing, resonant column, and in situ methods, illustrating these with sample data. Prediction draws must be done on both analytical and finite-element techniques to illustrate the critical speed, the bow-wave effect, in order to show how it is influenced by resilient modulus. Modeling reveals the available relationships, and their limitations, for deriving subgrade stiffness in this dynamic situation. Afterwards, this data may be used to define the relevant effects of resilient modulus values on design problems.

4. Case Study

Analysis of a simply supported pretensioned beam subjected to the effects of a high-velocity train going through it. The bridge will be a 100-feet single span beam, made out of four prestressed concrete beams placed in parallel.

The train transmits vertical loads at the point of contact of the wheels with the bridge. We assume the worst loading scenario to take place when the train is over the bridge and covering the whole structure.

Two sets of loads like the one shown in the figure below represent the loadings transmitted to the bridge from the wheels.

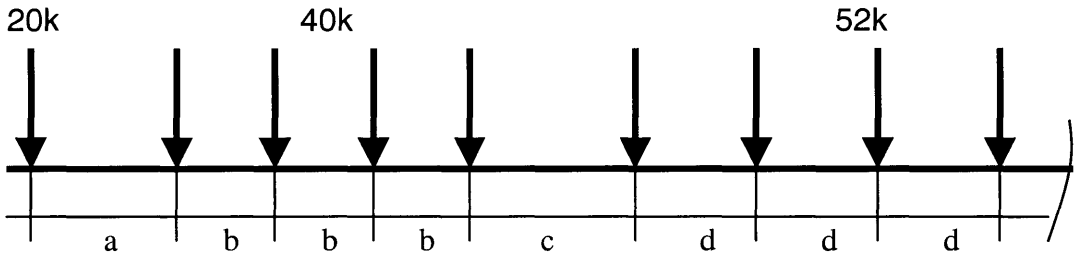

a	b	c	d
8	5	8	7

Distances in ft, loads in kips

The prestressed concrete has a cylinder strength of $5{,}000\frac{lb}{ft^2}$ and the steel for the prestressing of the beams will be a seven-wire standard strand Grade-270.

ACI 318 Building Code allowable stresses will be used for the analysis.

4.1. The objectives of the analysis are:

1. **Service Load Design of the pretensioned beam**

2. **Service Deflection Design**

The study of the deflections, the simply supported beam is subjected to, is the main purpose of this study. Two different analysis will be performed:

- **Static loading induced deflections**, at the beam midpoint, from the element self-weight and the railway instrumentation related dead load.

- **Dynamic deflections** induced by the train moving over the bridge will also be determined. The loading from the high-speed vehicle is transmitted to the structure in different places, corresponding to the wheel locations when the whole train is over the system. Those vertical displacements, at the beam midpoint, will be statically determined and increased by a dynamic impact ratio that takes into consideration the effects of the train moving loads.

  Since the study of the dynamic effect of the train moving over the bridge is the main purpose of this thesis, a more detailed analysis of it will be performed taking into consideration the sensitivity of behavior influencing variables such as the velocity of the train, the span of the bridge and the frequency of the loading induced by the vehicle.

4.1.1. Solution

4.1.1.1. Service Load Design

The span of each of the four beams of the bridge will be as mentioned above

$$L = 75\,ft = 900in$$

The loads that the structure will be carrying are

The assumed load corresponding to the weight of the railway infrastructure

$$w_L = 100\frac{lb}{ft} = 25.0\frac{lb}{in}$$

The living load transmitted to the bridge through the train wheels is described in the figure 1.1. Each beam will be carrying half of every concentrated load.

The properties of the concrete to be used for the beam are the following:

The concrete cylinder strength $f'_c = 5{,}000\frac{lb}{in^2}$

The concrete strength at transfer $f'_{ci} = 0.75 \cdot f'_c = 0.75 \cdot 5{,}000\frac{lb}{in^2} = 3{,}750\frac{lb}{in^2}$

The stress relieved tendons $f_{pu} = 270{,}000\frac{lb}{in^2}$

Time dependent losses of the initial prestress γ is assumed to be approximately *18%*

Then the ratio of initial prestress remaining after time dependent losses will be

$$\gamma = \frac{100 - 18}{100} = 0.82$$

The maximum allowable compressive stress in concrete immediately after transfer and prior to losses is

$$f_{ci} = 0.60 \cdot f'_{ci} = 0.60 \cdot 3750 \frac{lb}{in^2} = 2{,}250 \frac{lb}{in^2}$$

The maximum allowable compressive stress in concrete after losses at service-load level is

$$f_c = 0.45 \cdot f'_c = 0.45 \cdot 5000 \frac{lb}{in^2} = 2{,}250 \frac{lb}{in^2}$$

The maximum allowable tensile stress in concrete immediately after transfer and prior to losses is

$$f_{ti} = 3\sqrt{f'_{ci}} = 3 \cdot \sqrt{2{,}250} \frac{lb}{in^2} = 142.3 \frac{lb}{in^2}$$

This value may be increased to $6\sqrt{f'_{ci}}$ at the supports for simply supported members, as it is our case

$$f_{ti} = 6\sqrt{f'_{ci}} = 284.6 \frac{lb}{in^2}$$

The bending moments induced to the midpoint of the beam, where they get maximum values, due to the different loading effects are

Bending moment M_{Ins}, due to the dead load from the railway related infrastructures. This infrastructures are the rails, bolt connections, etc.

$$M_{Ins} = \frac{w_{Ins} \cdot L^2}{8} = \frac{25 \cdot 900^2}{8} = 843{,}800 lb \cdot in$$

Bending moment M_{Beam} due to the distributed self-weight of the beam

$$M_{Beam} = \frac{w_{Beam} \cdot L^2}{8} = \frac{67.91 \cdot 900^2}{8} = 9{,}541{,}000 lb \cdot in$$

The moment M_{Train} is produced by the train induced live load applied at several different locations. The positions of application of those loads, transmitted to the bridge through the train wheels, are shown in figure 1.1 at the midspan.

Load location (in.)	900	828	783	738	702	621	576	531	648
Moments (in. kip)	750	1,860	2,085	2,310	2,490	1,881	2,028	2,174	1,794

Load location (in.)	552	456	396	336	276	168	108	48
Moments (in. kip)	1,380	2,280	990	840	1,380	546	351	156

Since the tendon is harped, the critical section is close to the midspan, where dead-load and superimposed dead-load moments reach their maximum.

$$S^t \geq \frac{(1-\gamma) \cdot M_{Beam} + M_{train} + M_{Inst}}{\gamma \cdot f_{ti} - f_c}$$

$$= \frac{(1-0.82) \cdot 6{,}877{,}000 + 25{,}296{,}000 + 843{,}000}{0.82 \cdot 15.31 - 15.625}$$

$$= 11{,}400 in^3$$

$$S_b \geq \frac{(1-\gamma) \cdot M_{Beam} + M_{train} + M_{Inst}}{\gamma \cdot f_{ti} - f_c}$$

$$= \frac{(1-0.82) \cdot 6{,}877{,}000 + 25{,}296{,}000 + 843{,}000}{425 - 0.82 \cdot 2{,}250}$$

$$= 12{,}060 in^3$$

From the PCI design Handbook, we select a AASHTO Section Type 5 since it has the bottom-section modulus value S_b closest to the required value.

The Section properties of the concrete are as follows:

$A_s = 1{,}013 in^2$

$I_c = 521{,}180 in^4$

$W_d = 94.23 \frac{lb}{in}$

$c_t / c_b = 31.04 / 31.96 in$

$S^t = 16{,}790 in$

$S_b = 16{,}307 in$

$e_c = 28.99 in$

$e_e = 19.24 in$

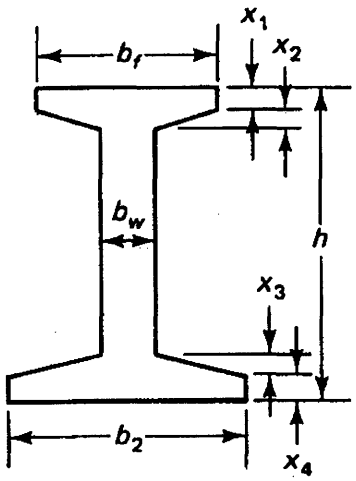

Actual I sections

Figure 3.7

The actual weight of the section is higher than the assumed value for the previous calculation

The new values for the section modulus are

$S^t = 11{,}600 in^3 < 16{,}790 in^3$

$S_b = 12{,}280 in^3 < 16{,}307 in^3$ *(Chosen section still valid.)*

Design of Strands and Check of Stresses

$$f_{pi} = 0.70 \cdot 270{,}000 = 189{,}000 psi$$

$$f_{pe} = 0.82 \cdot f_{pi} = 0.82 \cdot 189{,}000 = 154{,}980 psi$$

a) <u>Analysis of Stresses at Transfer.</u>

$$f^t = -\frac{P_i}{A_c}\left(1 - \frac{e_c c_t}{r^2}\right) - \frac{M_{Beam}}{S^t} \leq f_{ti} = 184 psi$$

$$184 = -\frac{P_i}{1{,}013}\left(1 - \frac{28.99 \cdot 31.04}{21.64^2}\right) - \frac{9{,}541{,}000}{16{,}790}$$

$$P_i = 908{,}100 lb$$

The required number of tendons will be, considering Grade 270 seven-wire standard strand, *0.6 in.* nominal diameter,

$$n_s = \frac{P_i}{A_s \cdot F_{pi}} = 22.557 \qquad \text{with} \qquad A_s = 0.213 in^2$$

We will try *20 – 0.6* in tendons for the standard section

$$A_{ps} = 20 \cdot 0.213 = 4.26 in^2$$

$$P_i = A_{ps} \cdot f_{pi} = 805{,}100 lb$$

$$P_e = A_{ps} \cdot f_{pe} = 660{,}200 lb$$

b) <u>Analysis of the final stresses at service load at the beam midspan</u>

The total moment at the midspan is

$$M_T = M_{Beam} + M_{Train} + M_{Ins} = 35{,}680{,}000 lb \cdot in$$

The stress transferred at that location is

$$f^t_{midspan} = \frac{-P_e}{A_c}\left(1 - \frac{e_c \cdot c_t}{r^2}\right) - \frac{M_T}{S^t} = -1{,}578 psi < 2{,}250 psi = f_c \quad \underline{OK}$$

$$f^b_{midspan} = \frac{-P_e}{A_c}\left(1 + \frac{e_c \cdot c_b}{r^2}\right) + \frac{M_T}{S_b} = -421.2 psi < 424.3 psi = f_t \quad \underline{OK}$$

c) Analysis of stresses at support section

The bending moment at the supports is zero.

$$f_{ti} = 6\sqrt{f'_{ci}} = 6\sqrt{3{,}750} = 367.4 psi$$

$$f_t = 6\sqrt{f'_c} = 6\sqrt{5{,}000} = 424.3 psi$$

At transfer the stresses are

$$f^t_{\sup port} = \left[\frac{-P_i}{A_c}\left(1 - \frac{e_e \cdot c_t}{r^2}\right)\right] = 199.2 psi < 367.4 psi = f_{ti} \qquad \textit{(Tension)} \ \underline{OK}$$

$$f^b_{\sup port} = \left[\frac{-P_i}{A_c}\left(1 + \frac{e_e \cdot c_b}{r^2}\right)\right] = -1{,}673 psi < -2{,}250 psi = f_{ci} \quad \textit{(Compression)} \ \underline{OK}$$

We set the apply a partial prestressing in the beams limiting the tensile stress in the concrete to a certain number. By doing this we will be improving performance, reducing cost by using a lower amount of prestress. Fully prestressed beams may exhibit an undesirable amount of upward camber because of the eccentric prestressing force, a displacement that is only partially counteracted by the gravity loads producing downward deflection. This tendency is aggravated by creep in the concrete, which magnifies the upward displacement due to the prestress force, but has little influence on the downward deflection due to live loads, which may be only intermittently applied.

Cracks may form occasionally, when full service load is applied, but these will close completely when that load is removed.

4.1.1.2. Analysis of deflections at beam midspan

4.1.1.2.1. Static loading induced deflections

We proceed with the analysis of the deflections produced on short-term for a cracked prestressed concrete beam, what means that the member we are designing will have the tension stresses limited to a certain value and therefore cracks will appear.

The deflection and camber at transfer at midspan due to a single harp or depression of the prestressing tendon is

$$\delta_{pi} = \frac{P_i e_c L^2}{8EI} + \frac{P_i (e_e - e_c)}{24EI}$$

with

$$E_c = 57{,}000\sqrt{f'_c} = 4{,}030{,}000\,psi$$

$$\delta_{pi} = \frac{908{,}100 \cdot 28.99 \cdot 900^2}{8 \cdot 3{,}490{,}000 \cdot 521{,}180} + \frac{908{,}100 \cdot (28.99 - 19.24) \cdot 900^2}{24 \cdot 3{,}490{,}000 \cdot 521{,}180} = \underline{1.95in} \uparrow$$

The deflection due to the beam self-weight is

$$\delta_{self-weight} = \frac{5 \cdot (94.23 + 8.33)}{384 \cdot 3{,}490{,}000 \cdot 521{,}180} = \underline{0.48in} \downarrow$$

We will limit the tensile stress to 750 psi at the midspan bottom fibers at service load. The tensile stress exceeding the modulus of rupture is

$$f_r = 7.5 \cdot \sqrt{f'_c} = 530\,psi$$

The net tensile stress beyond the first cracking load at the modulus of rupture is

$$f_{net} = f_b - f_r = 750 - 530 = 220\,psi \quad \textit{(TENSION)}$$

The portion of the moving load that would not result in tensile stress at the bottom fibers is the corresponding to

$$k = \frac{585 - 220}{585} = 0.623$$

with $f_b = 585\,psi$ being the stress at the bottom fiber of the beam

and the deflection at that point is

$\delta_g = k \cdot \delta_{Train}$ with $\delta_{Train} = 0.313in$

$\delta_g = 0.623 \cdot 0.313 = 0.195in \downarrow$

when the δ_g deflection is overpassed cracks will appear at the beam bottom fibers.

Using the effective moment of inertia I_e method we will determine the static deflection due to the live load from the train going through the beam

$$I_e = \left(\frac{M_{cr}}{M_a}\right)^3 I_g + \left[1 - \left(\frac{M_{cr}}{M_a}\right)^3\right] I_{cr} \le I_g \qquad I_g = I_c = 521{,}180in^4$$

$$\left(\frac{M_{cr}}{M_a}\right) = 1 - \left(\frac{f_{tl} - f_r}{f_L}\right)$$

with

$f_{tl} = 750psi$ final total stress

$f_r = 530psi$ modulus of rupture

$f_L = 585psi$ live load stress

solving for I_e we first calculate the critical moment of inertia

$$I_{cr} = n_p A_{ps} d_p^2 (1 - 1.6\sqrt{n_p \rho_p}) = 79{,}980in^4$$

$$I_e = 187{,}400in^4$$

and the static deflection due to live load is $\delta_L = \underline{0.77in} \downarrow$

4.1.1.2.2. Dynamic deflections

We will perform the analysis of the dynamic behavior of the prestressed concrete beam. In order to do it we will be considering the midspan point since it is the most critical one due to the superposition of dead load, beam self-weight and the effects of the train over the bridge.

The vertical effects from the vehicle on the beam results in an increase or decrease of bridge deformations comparing to the ones from the static loading effects. A design practice procedure is to consider a static effect multiplier factor which states how many times it has to be increased in order to cover the additional dynamic loads. This factor is very simple and does not take into account most of the parameters which influence the dynamic behavior of the structure. However, the factor is accurate enough as for ensuring the safety and reliability of this types of bridges.

We will consider several loadings applied from the train to the beam when the vehicle covers totally the structure. Neglecting damping and assuming the simplified shape function of the beam deformation to be equal to the first mode of vibration, we will determine an equation for the deflection at midspan as a function of time.

Then we will determine the dynamic impact ratio that reduces of magnifies the static deflection of the structure at the selected midpoint. The velocity of the train has an important influence on the dynamic response; therefore, the critical one at which it is maximum, will be as well determined.

The conclusion of this dynamic study is to be able to determine if the high velocity loading effect is a determinant factor in the design and in case it is, what is the influence on the cost of the structure.

First we will determine the generalized mass, generalized stiffness and natural frequency of the system

$$\psi(x) = \frac{\sin \pi x}{L} \qquad \psi''(x) = -\frac{\pi^2}{L^2} \sin \frac{\pi x}{L} \text{g}$$

$$\tilde{m} = \int_0^L m \sin^2 \frac{\pi x}{L} dx = \frac{mL}{2}$$

$$\tilde{k} = \int_0^L EI \left(\frac{\pi^2}{L^2} \right)^2 \sin^2 \frac{\pi x}{L} dx = \frac{\pi^4 EI}{2L^3}$$

$$\omega_n = \sqrt{\frac{\tilde{k}}{\tilde{m}}} = \frac{\pi^2}{L^2} \sqrt{\frac{EI}{m}}$$

This happens to be the exact value of the lowest natural frequency of the bridge because, as mentioned above, the $\psi(x)$ selected is the exact shape of the fundamental natural vibration mode of a simply supported beam.

Now we will determine the generalized force. A load P traveling with a velocity v takes time $t_d = \frac{L}{v}$ to cross the bridge. At any time t the dynamic impact of the loading excitation is shown for several different velocities at the end of the dynamic study.

The moving load can be described mathematically as

$$p(x,t) = \begin{cases} p\delta(x - vt) & 0 \le t \le t_c \\ 0 & t \ge t_d \end{cases}$$

where $\delta(x-vt)$ is the Dirac delta function centered at $x = v \cdot t$; it is a mathematical description of the traveling concentrated load. The generalized force is

$$\tilde{p}(t) = \int_0^L p(x,t)\psi(x)dx = \int_0^L p\delta(x-vt)\sin(\pi x/L)dx$$

$$\tilde{p}(t) = \begin{cases} p\sin(\pi vt/L) & 0 \le t \le t_c \\ 0 & t \ge t_d \end{cases}$$

This generalized force is a half-cycle sine pulse.

We will solve now the equation of motion

$$\tilde{m}\,\ddot{z} + \tilde{k}\,z = \tilde{p}(t)$$

The defined generalized equations describe the response of a single degree of freedom system to a half-cycle sine pulse. This solution will be considered to the bridge problem by changing the notation from u(t) to z(t), that refers to the vertical displacements at the bridge and noting that

$$t_d = \frac{L}{v} \qquad T_n = \frac{2\pi}{\omega_n} \qquad (z_{st})_0 = \frac{p}{\tilde{k}} = \frac{2p}{mL\omega_n^2}$$

The results will be

$$z(t) = \frac{2p}{mL}\frac{1}{\omega_n^2 - (\pi v/L)^2}\left(\sin\frac{\pi vt}{L} - \frac{\pi v}{\omega_n L}\sin\omega_n t\right) \qquad t \le L/v$$

$$z(t) = -\frac{2p}{mL}\frac{(2\pi v/\omega_n L)\cos(\omega_n L/2v)}{\omega_n^2 - (\pi v/L)^2}\sin\omega_n(t - L/2v) \qquad t \geq L/v$$

The response is given by the first of the last two equations above while the moving load is on the bridge span. The second of the equations gives the response after the load has crossed the span.

The deflection at the beam midspan will be for a certain load

$$u(x,t) = z(t)\psi(x) = z(t)\sin\frac{\pi x}{L}$$

at midspan $x = \frac{L}{2}$ $\qquad u\left(\frac{L}{2},t\right) = z(t)$

The numerical results for the given prestressed-concrete structure and different vehicle speeds is

E modulus	4031000	psi
Effective mom Inertia	187400	In^4
Span of beam	900	in
Length	75	ft
mass per in	5.7	lb/in
section mass	94.23	lb/ft
natural frequency	4.452	rad/sec
natural period	1.411	sec
load frequency	0.096	rad/sec
time to pass through	32.72	sec

The position of the load traveling with a velocity v crossing the midspan point of the bridge will have a vertical displacement position as the ones in the graphics 1 to 5 shown below.

For velocity *v = 1* mph

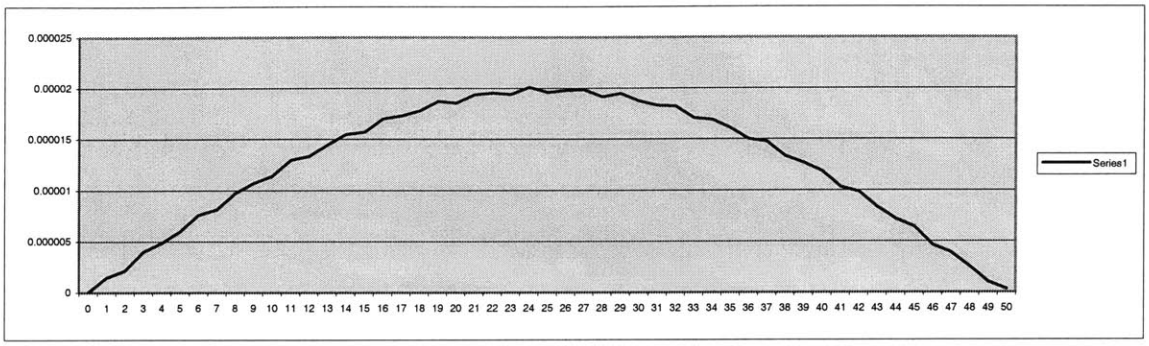

For velocity *v = 30* mph

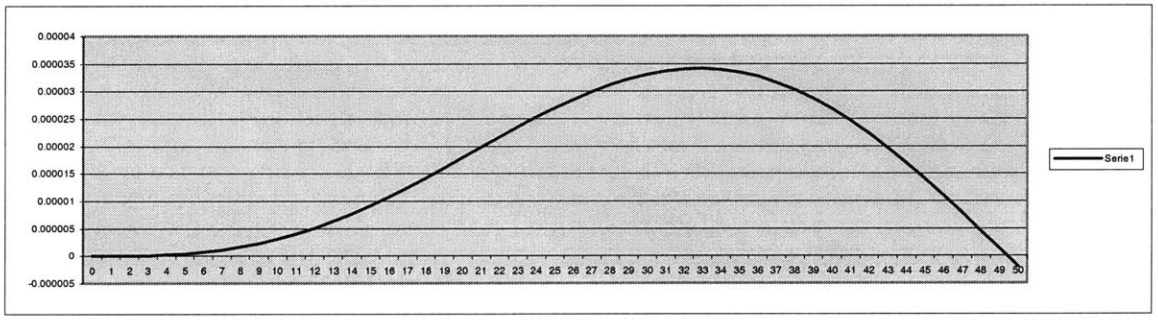

For velocity *v = 70* mph

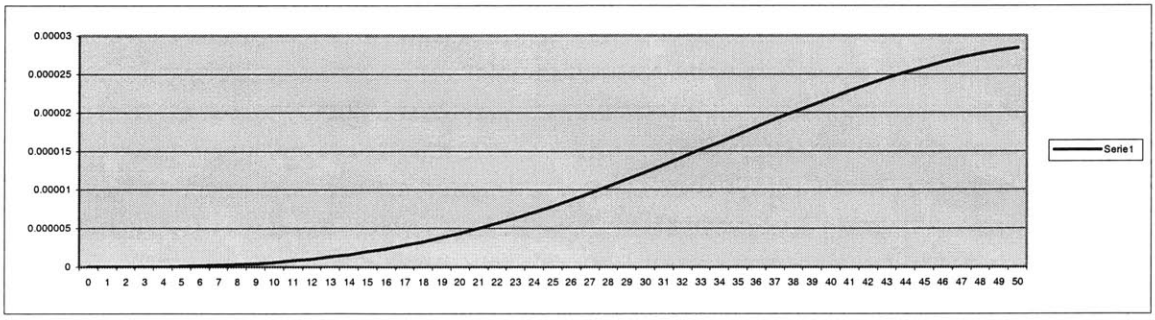

For velocity *v = 100* mph

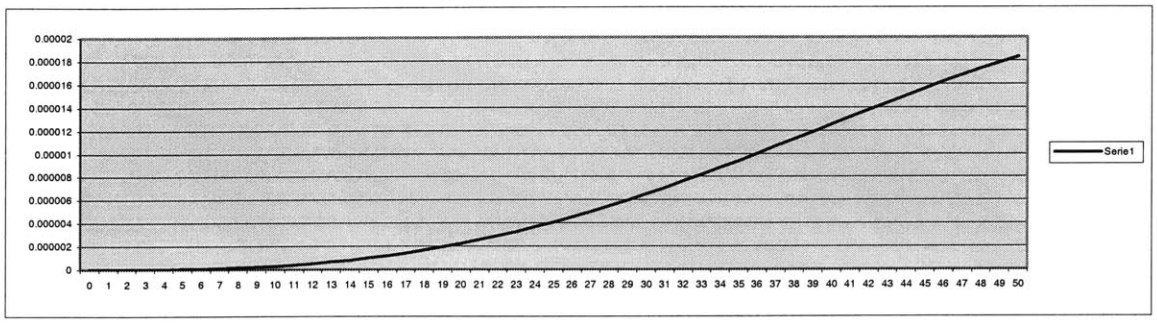

For velocity v = 150 mph

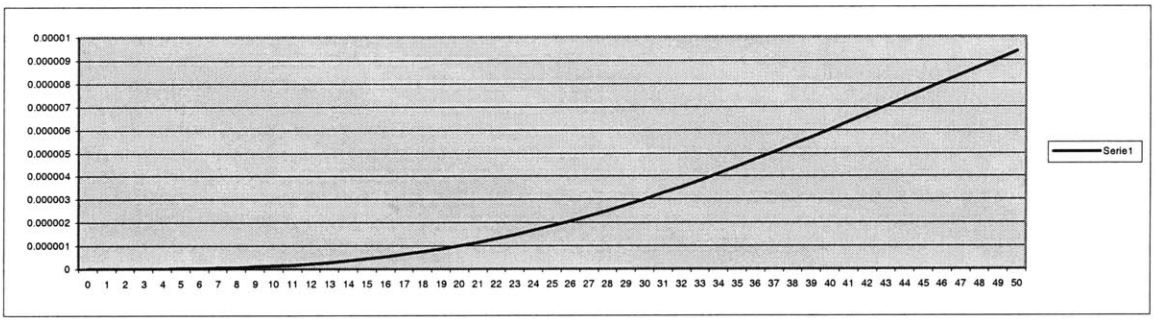

For velocity *v = 180* mph

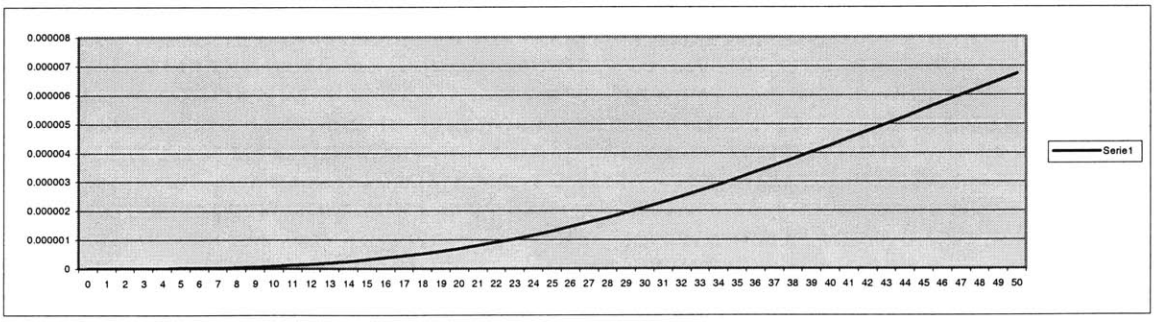

For velocity $v = 210$ mph

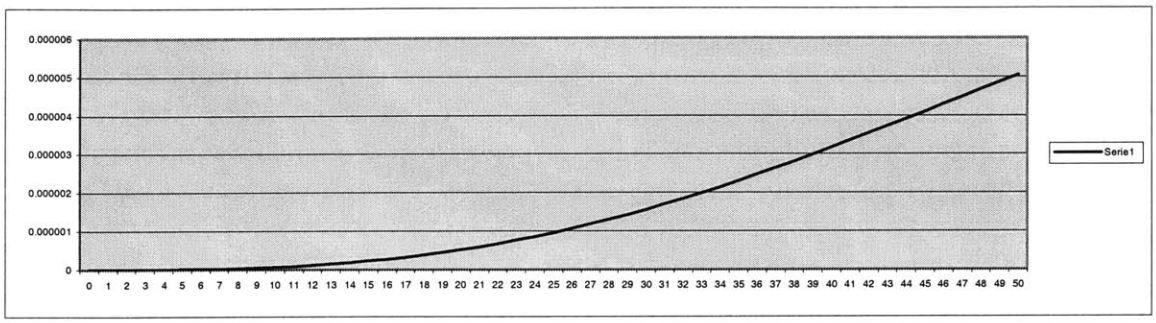

The may easily appreciate with these graphical results is that as the velocity increases the maximum displacement of the midspan is produced by the load applied closer to the right support.

The static response at the midspan point of the bridge will have the position, due to the vertical deflection, corresponding to the shape graphed below.

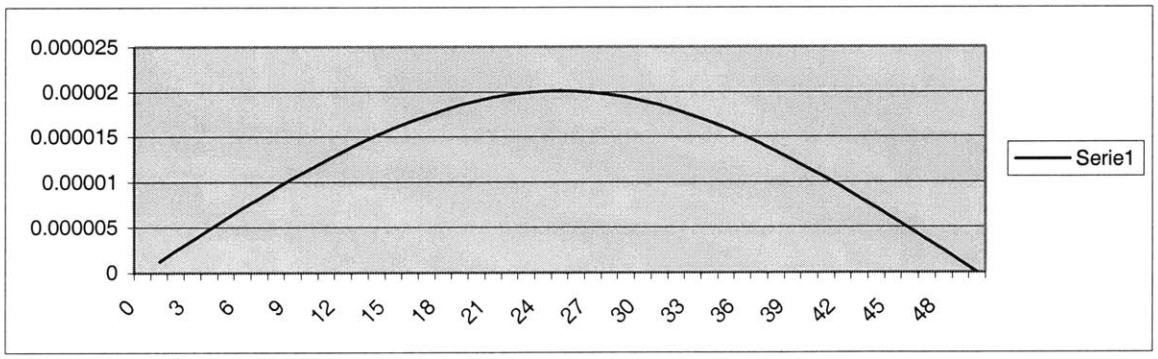

4.1.1.2.3. Dynamic Impact Ratio

The dynamic amplification factor is the ratio between the dynamic and the static response. Therefore, the one corresponding to the analysis of the midspan point for a certain range of load frequencies will be

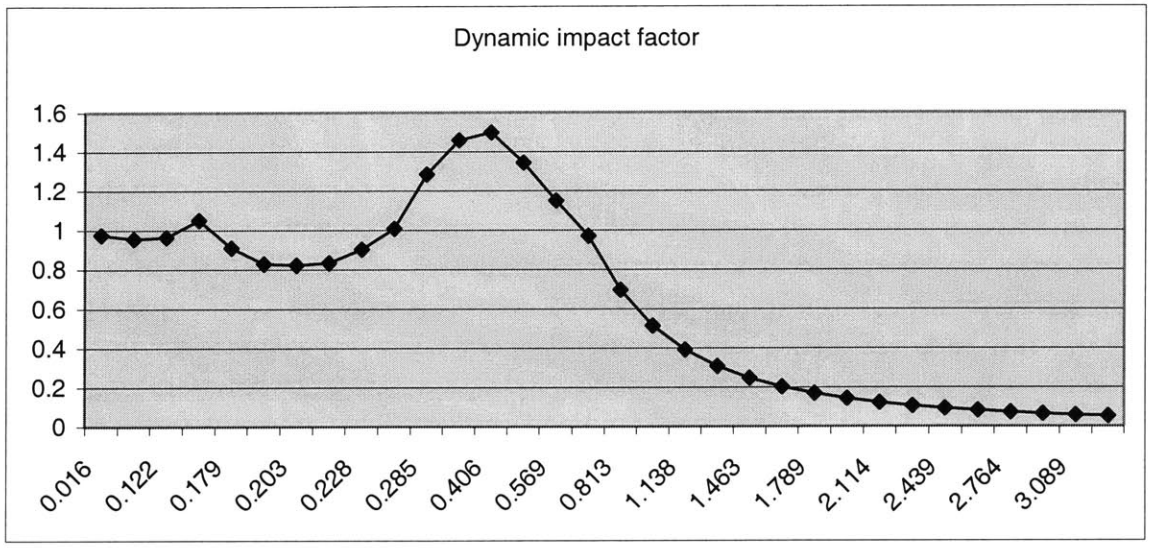

We may appreciate the similarity in the behavior of the response with the results obtained for a single degree of freedom analysis.

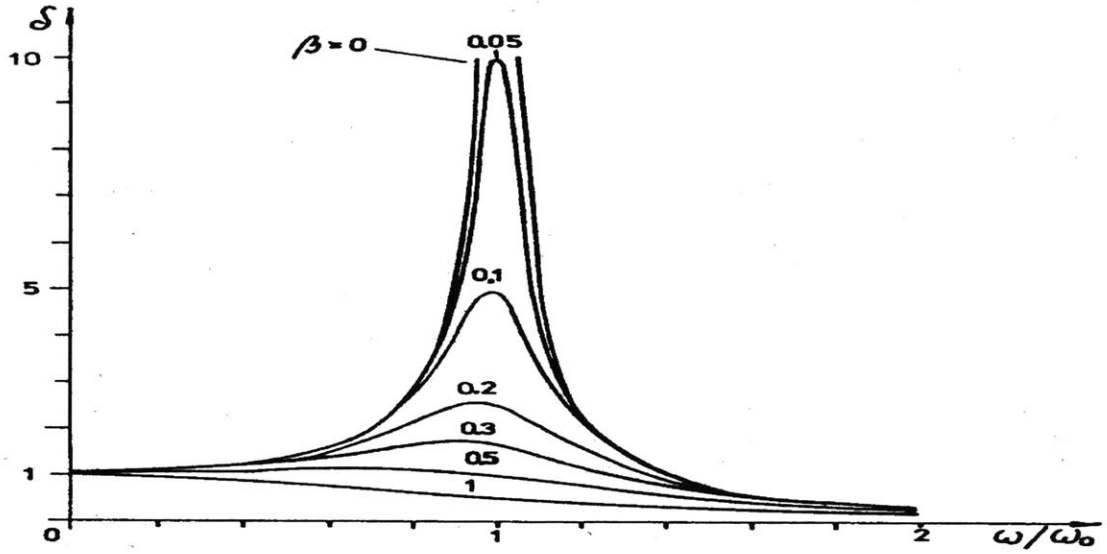

A much larger number of data would make would provide smoother dynamic impact ratio curvs. However, it is good enough to stablish the similarity and to be able

to develop conclusions on the dynamic behavior of the beam due to the high-velocity train crossing.

We will calculate the dynamic deflection of the midspan for the critical velocity, which happens for the resonance loading excitation. The dynamic factor at this point is 1.498 times the deflection at the midspan for the static loading. The static deflection is 0.7708 inches.

$$\delta_{dyn} = 1.498 \cdot 0.7708 = 1.154in \downarrow$$

With the deflections due to the prestressing and self-weight and dead load of the railway instrumentation calculated before

$$\delta_{camber} = 1.95in \uparrow$$
$$\delta_{self-weight} = 0.48in \downarrow$$

Then the final maximum negative displacement that the prestressed concrete beam will experiment at the midspan point will be:

$$\delta_{beam} = 0.315in$$

The code stablishes that the maximum deflection for this type of structures should not exceed *L/800*, which for the *75 ft* span beam is *1.125 in*. The design of the beam for dynamic deflection amplification is then correct.

References

1. **Deflection ordinates for single-span and continuous beams.** Georg Anger and Karl Tranmm. New York1965
2. **Bridge engineering : design, rehabilitation, and maintenance of Bridges.** Tonias, Demetrios E. New York 1995
3. **Dynamics of structures**. Anil K. Chopra, University of Berkeley. New Jersey 1995
4. **High Performance Maglev Guideway Design**. Scott Phelan, PhD Thesis. Massachusetts Institute of Technology. January 1993.
5. **Transportation Vehicle/Beam Elevated Guideway Dynamic Iterations.** Richardson and Wormley 74. "A state of the art review". Journal of Dynamic Systems, Measurement and Control. ASME, P1-11 (1974)
6. **Obras Publicas: Revista del Colegio de Ingenieros de Caminos, Canales y Puertos.** "Los puentes del futuro. Angel Aparicio Bengoechea. ". N 20 / Verano 1991, P 6 – 21
7. **Obras Publicas: Revista del Colegio de Ingenieros de Caminos, Canales y Puertos**. "Puentes de hormigón pretensado para lineas ferroviarias de Alta Velocidad". Reiner Saul. N 20 / Verano 1991, P 40 - 51
8. **Dynamic Response of elevated High-speed railway.** Yung-Hsiang Chen and Chen-Yu Li. Journal of Bridge Engineering. May 2000. Pg 124-131.
9. **Design of Prestressed Concrete Structures.** T Y Lin / Ned H. Burns. Edit. Wiley, John & Sons Incorporated. November 1990
10. **Design of Prestressed Concrete.** Arthur H. Nilson. Edit. Wiley, John & Sons Incorporated. March 1987.
11. **Launched Bridges.** Marcho Rosignoli. June 1998
12. **The Cantilever Construction of Prestressed Concrete Bridges**. Jacques Mathivat. Edit. Wiley, John & Sons Incorporated. January 1984.

13. Dynamics of Railway Bridges. Ladislav Fryba. American Asociation of Civil Engineers. January 1996.

14. Structural Analysis: A Unified Classical and Matrix Approach. A Ghali , A. M. Neville. 3rd Edition, New York 1972.

15. Prestressed Concrete: A fundamental Approach. Edward G. Nawy. 2nd Edition, New Jersey 1995.